

Overcoming DoF Limitation in Robust Beamforming: A Penalized Inequality-Constrained Approach

Wenqiang Pu, Jinjun Xiao, *Member, IEEE*, Tao Zhang, *Member, IEEE*, Zhi-Quan Luo, *Fellow, IEEE*

Abstract—A well-known challenge in beamforming is how to optimally utilize the degrees of freedom (DoF) of the array to design a robust beamformer, especially when the array DoF is smaller than the number of sources in the environment. In this paper, we leverage the tool of constrained convex optimization and propose a penalized inequality-constrained minimum variance (P-ICMV) beamformer to address this challenge. Specifically, we propose a beamformer with a well-targeted objective function and inequality constraints to achieve the design goals. The constraints on interferences penalize the maximum gain of the beamformer at any interfering directions. This can efficiently mitigate the total interference power regardless of whether the number of interfering sources is less than the array DoF or not. Multiple robust constraints on the target protection and interference suppression can be introduced to increase the robustness of the beamformer against steering vector mismatch. By integrating the noise reduction, interference suppression, and target protection, the proposed formulation can efficiently obtain a robust beamformer design while optimally trade off various design goals. When the array DoF is fewer than the number of interferences, the proposed formulation can effectively align the limited DoF to all of the sources to obtain the best overall interference suppression. To numerically solve this problem, we formulate the P-ICMV beamformer design as a convex second-order cone program (SOCP) and propose a low complexity iterative algorithm based on the alternating direction method of multipliers (ADMM). Three applications are simulated to demonstrate the effectiveness of the proposed beamformer.

Index Terms—Array signal processing, robust beamforming, degrees of freedom, convex optimization

I. INTRODUCTION

Beamforming is a fundamental technique in array signal processing, which exploits the spatial degrees of freedom (DoF) to enhance the desired signal and suppress undesired interferences and noise. The beamforming technique has been widely used in many multi-channel signal processing areas, i.e., wireless communication [3], microphone array speech

processing [4], radar [5], sonar [6], medical imaging [7], and etc. The key procedure in beamforming is specifying the so called *beamformer*, which serves as a complex coefficient vector to linearly combine signals received by array elements. In the past decades, various beamformer design criteria has been extensively studied, these criteria can be divided into two types: data-independent and data-dependent criteria. The performance of data-independent beamformers [8]–[10] is limited due to the missing knowledge of the signal environment. Instead, the data-dependent beamformers can deliver optimal performance due to their adaptivity to the signal environment statistics and, as such, they are also referred as adaptive beamformers. One representative adaptive beamformer is the minimum variance distortionless response (MVDR) beamformer [11], which has been widely used in applications due to its convenience of practical implementation as well as its theoretical guarantee to maximize the output signal-to-interference-and-noise-ratio (SINR).

However, the performance of the MVDR beamformer suffers a degradation due to the imperfect knowledge of practical environment, i.e., imprecise steering vectors (SV), finite number of snapshots, direction-of-arrival (DoA) errors, etc. Generally speaking, these imperfections lead to two types of model uncertainties of the MVDR beamformer. One uncertainty is the mismatch of SV of the target signal due to array calibration error and DoA error of the target signal. This can lead to inevitable distortion of the target signal. The other uncertainty lies in the estimation error of the covariance matrix of interference plus noise, which is often caused by the finite number of data samples, the presence of the target signal in the training samples, and the non-stationarity of signals. Such uncertainty can not only lead to a degradation on suppressing interference and noise, but also distort the target signal if it is present in the training data samples. Facing with the above two types of uncertainties, various robustness beamformers were proposed and studied in the past four decades, to mitigate the negative effects of one or both of the uncertainties.

A comprehensive review of the principles for minimum variance robust adaptive beamforming technique was reported in [12]. Here after, we briefly review several representative robust beamforming techniques. To handle the uncertainty of SV, the linearly constrained minimum variance (LCMV) beamformer [13] enforces multiple distortionless constraints on possible DoAs of the target signal. Though the LCMV beamformer stabilizes the mainlobe response for possible target DoAs, it does use up the DoF resource that could

Part of this work is presented in IEEE Workshop on Applications of Signal Processing to Audio and Acoustics (WASPAA), Oct. 2017 [1] and IEEE International Conference on Acoustics, Speech and Signal Processing (ICASSP), April 2018 [2]. This work is partially supported by a research gift from Starkey Hearing Technologies, the leading talents of Guangdong province Program (No. 00201501), the National Natural Science Foundation of China (No. 61731018), the Development and Reform Commission of Shenzhen Municipality, and the Shenzhen Fundamental Research Fund (No. KQTD201503311441545).

J. Xiao and T. Zhang are with Starkey Hearing Technologies, Minneapolis, MN 55455, USA. Email: jinjun_xiao, tao_zhang@starkey.com

W. Pu and Z.-Q. Luo are with The Chinese University of Hong Kong, Shenzhen, and Shenzhen Research Institute of Big Data, 518100, China. E-mail: puwenqiang, luozq@cuhk.edu.cn

be otherwise used for suppressing interference and noise. Instead of enforcing multiple equality constraints, uncertainty set based beamformers [14]–[17] model the mismatch part of the SV lies in a bounded spherical or ellipsoidal, where the mainlobe is stabilized by a worst-case optimization criterion [14]–[16] or by iteratively estimating the SV [17] from the uncertainty set. Another way for mitigating the uncertainty of SV is the eigenspace based beamformers [18]–[20], which modify the SV by projecting it onto the estimated signal-plus-interference subspace. The eigenspace based beamformers suffer from noise corrosion when signal-to-noise ratio (SNR) is low.

To handle the uncertainty of the covariance matrix, several robust techniques are proposed by reconstructing the sample covariance matrix. The well known one is the diagonal loading (DL) based beamformer [21]–[23], which modify the sample covariance matrix by adding a diagonal matrix. As the DL beamformer though only modifies the covariance matrix, it also enable to mitigate the impact of SV mismatch [15]. However, its performance may degrade in high SINR situation if the target signal is presented in training data samples. Recently, several covariance matrix reconstruction based beamformers were proposed [24]–[26], these beamformers exploit the a priori knowledge of the array manifold to reconstruct the interference-plus-noise covariance matrix and estimate the SV of the target signal. But the covariance matrix reconstruction procedure are based on integration operation over specified angle regions, which requires a large computation cost especially for large size array and 2-dimensional angle space.

In this paper, we utilize the convex optimization technique to revisit the robust beamformer design problem. We propose a penalized inequality-constraint minimum variance (P-ICMV) beamformer based on the min-max criteria and also develop an efficient optimization algorithm for solving the problem. We summarize our contributions as follows:

(1) Various robustness considerations: The P-ICMV beamformer is robust against three kinds of errors caused by different uncertainties in practice, including the DoA error, the SV mismatch error, and the covariance matrix estimation error. Precisely, two types of inequality constraints (one for preserving target signal and the other for suppressing interferences) for controlling spatial responses around different directions are introduced to provide robustness against DoA error. In the presence of SV mismatch, these inequality constraints also imply bounded spatial responses, and the impact of SV mismatch is controlled by controlling the ℓ_2 norm of beamformer. In addition, those inequality constraints for interference suppression further provide an efficient suppression guarantee when the covariance matrix of interference-plus-noise are badly estimated or even unavailable.

(2) Intelligent DoF allocation: To allow a feasible beamformer design under various robustness considerations, the P-ICMV beamformer utilizes a penalization strategy to intelligently allocate the limited array DoF. By penalizing different terms in the objective of the P-ICMV formulation, the limited array DoF can be intelligently allocated for achieving noise reduction, interference suppression and target protection with robustness. Specifically, the spatial responses on all possible

directions of interferences are penalized, enabling the P-ICMV beamformer to handle any number of interferences with robustness. In particular, the number of inequality constraints for suppressing interferences is no longer limited by the array DoF. In addition, the worst-case distortion of the target signal is bounded by the proposed inequality constraints. By aligning different values of the pre-defined parameters, different priorities among noise reduction, interference suppression and target protection can be achieved.

(3) Flexible robustness adjustment: From the point of dealing with different kinds of robustness situations, the P-ICMV beamformer contains a set of user-specified parameters which allow a flexible robust beamformer design. Specifically, different levels of DoA errors can be handled by specifying the sizes of angle regions covered by inequality constraints, different allowable target signal distortions can be controlled by the parameters in target protection inequality constraints, different suppressing preferences among interferences can be achieved by adjusting parameters involved in the min-max criterion, and different levels of array calibration errors can be dealt by controlling the ℓ_2 norm of beamformer.

(4) An efficient optimization algorithm: From the optimization point of view, the P-ICMV formulation is a convex second order cone programming (SOCP), which can be solved by the well known interior point method [27]. However, facing with the rapid progress of digital technique, beamforming with a large-size array or limited computation capacity arise in lots of applications and computationally more efficient optimization algorithm is necessary. Hence, we also develop a low complexity iterative algorithm based on the alternating direction method of multipliers (ADMM) algorithm for solving the P-ICMV formulation. Compared to the interior point method which has a computation complexity in the a polynomial order of array size, the developed algorithm only requires a computation complexity of quadratic order per iteration.

We adopt the following notations in this paper. Lower and upper case letters in bold are used for vectors and matrices respectively. For a given matrix \mathbf{X} , we denote its transpose and Hermitian transpose by \mathbf{X}^T and \mathbf{X}^H respectively. If \mathbf{X} is a square matrix, we use $\lambda_{\min}(\mathbf{X})$ and $\lambda_{\max}(\mathbf{X})$ to denote its smallest and largest eigenvalue respectively, use $\mathbf{X} \succ \mathbf{0}$ ($\mathbf{X} \succeq \mathbf{0}$) to denote that it is a positive definite (semi-definite) matrix, and use \mathbf{X}^{-1} to denote its inverse (if exists). For a given complex number c , we use $\text{Re}\{c\}$ and $\text{Im}\{c\}$ to denote its real part and imaginary part respectively, and use $\angle c$ to denote the angle of c . We use $\|\mathbf{x}\|$ to denote Euclidean (ℓ_2) norm of the vector \mathbf{x} . $\mathbb{E}[\cdot]$ is used to represent the expectation operation. The notation \mathbf{I} represents the identity matrix with an appropriate size, and the M -dimensional real (complex) vector space is denoted by \mathbb{R}^M (\mathbb{C}^M).

II. SIGNAL MODEL

Consider an array with M omni-directional array elements. There are $K + 1$ statistically independent narrow-band signal sources at different directions θ_k , $k = 0, 1, \dots, K$ ($\theta_k \neq$

$\theta_{k'}, \forall k \neq k'$). The signals received by the array at time $n = 1, 2, \dots$, can be modeled as,

$$\mathbf{x}(n) = s_0(n)\mathbf{a}_{\theta_0} + \sum_{k=1}^K s_k(n)\mathbf{a}_{\theta_k} + \mathbf{v}(n) \in \mathbb{C}^M, \quad (1)$$

where $s_k(n) \in \mathbb{C}$ is the k -th source signal at discrete time instance n , $\mathbf{a}_{\theta_k} \in \mathbb{C}^M$ is the SV associating with direction θ_k , and $\mathbf{v}(n) \in \mathbb{C}^M$ is the noise. Suppose $s_0(n)$ is the target signal and others are unwanted signal, (1) can be simplified as

$$\mathbf{x}(n) = s_0(n)\mathbf{a}_{\theta_0} + \mathbf{u}(n) \in \mathbb{C}^M, \quad (2)$$

where $\mathbf{u}(n) = \sum_{k=1}^K s_k(n)\mathbf{a}_{\theta_k} + \mathbf{v}(n)$ is the unwanted signal. The beamforming technique linearly combines $\mathbf{x}(n)$ by a so-called beamformer $\mathbf{w} \in \mathbb{C}^M$ such that the beamforming output signal

$$z(n) = \mathbf{w}^H \mathbf{x}(n) \quad (3)$$

satisfies a specified requirement, e.g., maximize the signal-to-interference plus noise ratio (SINR) of $z(n)$.

With the *a priori* knowledge of the target signal's SV \mathbf{a}_{θ_0} , the well-known MVDR beamformer attempts to minimize the undesired signal power at beamforming output subject to a distortionless constraint on the array response at direction θ_0 . The MVDR beamformer formulation is

$$\min_{\mathbf{w}} \mathbb{E} [|\mathbf{w}^H \mathbf{u}(n)|^2] \quad (4a)$$

$$\text{s.t. } \mathbf{w}^H \mathbf{a}_{\theta_0} = 1. \quad (4b)$$

Linear constraint (4b) guarantees $s_0(n)$ being preserved in $z(n)$ without any distortion and the objective function in (4a) can be further expressed as

$$\mathbb{E} [|\mathbf{w}^H \mathbf{u}(n)|^2] = \mathbf{w}^H \mathbf{R}_u \mathbf{w}, \quad (5)$$

where $\mathbf{R}_u \triangleq \mathbb{E} [\mathbf{u}(n)\mathbf{u}^H(n)]$ is the covariance matrix of $\mathbf{u}(n)$. By the Lagrange multiplier method [28], the optimal solution of problem (4) is

$$\mathbf{w}^* = \frac{\mathbf{R}_u^{-1} \mathbf{a}_{\theta_0}}{\mathbf{a}_{\theta_0}^H \mathbf{R}_u^{-1} \mathbf{a}_{\theta_0}}. \quad (6)$$

Though the MVDR beamformer \mathbf{w}^* theoretically guarantees a maximal SINR at the beamforming output [29], its performance could degrade significantly in practice due to:

(1) Inaccuracy of \mathbf{R}_u : The exact covariance matrix \mathbf{R}_u is usually unavailable in most applications and it usually requires to be estimated from finite N training data samples. Several covariance matrix estimation approaches [21]–[26] were proposed to reduce the estimation error or improve the robustness against the imprecise knowledge of the statistic property of the undesired signal $\mathbf{u}(n)$.

(2) Mismatch of \mathbf{a}_{θ_0} : Linear constraint (4b) is motivated by the array signal model (2) to preserve $s_0(n)$ in $z(n)$ without distortion. In practice, \mathbf{a}_{θ_0} needs to be estimated and can be inaccurate. The mismatch of \mathbf{a}_{θ_0} would lead to undesirable target signal distortion. Further, together with the appearance of target signal in the training data samples, signal cancellation phenomenon [30] would bring a heavy target signal distortion.

Generally speaking, robustness against the mismatch of \mathbf{a}_{θ_0} has been widely studied in the past decades, which can be achieved by exploiting the *a priori* knowledge of \mathbf{a}_{θ_0} . However, robustness against the inaccuracy of \mathbf{R}_u is usually considered in an estimation or reconstruction manner [21]–[26], which relies on the interference-plus-noise data samples. Instead, the possibility and advantages of enforcing additional constraints for interference suppression with robustness require to be further explored. Suppressing interferences by proper inequality constraints not only provides robustness against the inaccuracy of \mathbf{R}_u , but also enables to design robust beamformers in sample-free situations where the estimation/reconstruction based beamformers are unable to handle. For example, interference suppression with only noise samples being available, or synthesizing beam pattern with prescribed nulls [31]. However, the major challenge for enforcing interference suppression constraints lies in the limitation of DoF provided by the array. For the LCMV beamformer or other linear constraints based beamformers [32], [33], the number of linear constraints in general should no more than the number of array elements; otherwise it render the optimization problem infeasible. Such limitation on the number of linear constraints blocks the further exploration of using linear constraints for interference suppression with robustness.

On the other hand, recent research [34], [35] in speech enhancement applications introduced the approach to relax the equality constraints into inequality ones, and proposed a so-named inequality constrained minimum variance (ICMV) beamformer. Although the ICMV beamformer may also be limited by the number of constraints, the flexibility of inequality constraints provides a potential way for overcoming limitation on the number of constraints. In the next section, we will present our proposed P-ICMV beamformer formulation, which includes two types of inequality constraints and a penalized objective function. A key advantage of P-ICMV beamformer is its ability to effectively handle arbitrary number of interferences with robustness on the best effort basis regardless of array DoF. Further, it also provides a flexible robustness adjustment to design beamformers for different situations.

III. PROPOSED P-ICMV BEAMFORMER DESIGN

To address the mismatch of SVs and inaccuracy of covariance matrix, we firstly introduce two types of inequality constraints in subsections III-A and III-B respectively. Then we propose a min-max criterion to deal with the limitation of DoF in subsection III-C, and the final P-ICMV beamformer formulation is given in subsection III-D.

A. Robustness against Steering Vector Mismatch

To handle the SV mismatch, we relax equality constraint (4b) into inequality version and control distortion within a certain level. Specifically, for a given direction θ , equality constraint $\mathbf{w}^H \mathbf{a}_{\theta} = 1$ is relaxed to

$$|\mathbf{w}^H \mathbf{a}_{\theta} - 1| + \delta \|\mathbf{w}\| \leq c_{\theta}, \quad (7)$$

where $c_\theta \geq 0$ is a user-defined tolerable distortion threshold with respect to θ and $\delta \geq 0$ is a pre-defined parameter for controlling the true spatial response. Notice that in the presence of SV mismatch,

$$\mathbf{a}_\theta = \bar{\mathbf{a}}_\theta + \Delta\mathbf{a}_\theta,$$

where $\bar{\mathbf{a}}_\theta$ is the true SV and $\Delta\mathbf{a}_\theta$ is the perturbation vector, precisely specifying the true spatial response $\mathbf{w}^H \bar{\mathbf{a}}_\theta$ is a difficult task as $\Delta\mathbf{a}_\theta$ is unknown. Unlike the worst-case optimization [14]–[16] or steering vector re-estimation [17] approaches where the true spatial response $\mathbf{w}^H \bar{\mathbf{a}}_\theta$ is uncontrollable. Inequality (7) implies a controllable target signal distortion, under a general assumption that the ℓ_2 norm of $\Delta\mathbf{a}_\theta$ is bounded, i.e., $\|\Delta\mathbf{a}_\theta\| \leq \delta$ with $\delta > 0$. The target distortion is represented in terms of $|\mathbf{w}^H \bar{\mathbf{a}}_\theta - 1|$ and its bound implied from (7) is given in Proposition 1.

Proposition 1. Suppose $\mathbf{a}_\theta = \bar{\mathbf{a}}_\theta + \Delta\mathbf{a}_\theta$, $\|\Delta\mathbf{a}_\theta\| \leq \delta$, and $|\mathbf{w}^H \mathbf{a}_\theta - 1| + \delta\|\mathbf{w}\| \leq c_\theta$, then $|\mathbf{w}^H \bar{\mathbf{a}}_\theta - 1| \leq c_\theta$.

Proof. By applying the triangle and the Cauchy–Schwarz inequalities, we can proof Proposition 1. We first apply the triangle inequality,

$$\begin{aligned} |\mathbf{w}^H \mathbf{a}_\theta - 1| &= |\mathbf{w}^H (\bar{\mathbf{a}}_\theta + \Delta\mathbf{a}_\theta) - 1| \\ &\geq |\mathbf{w}^H \bar{\mathbf{a}}_\theta - 1| - |\mathbf{w}^H \Delta\mathbf{a}_\theta|. \end{aligned} \quad (8)$$

Then, together with (8) and Cauchy–Schwarz inequality for $|\mathbf{w}^H \Delta\mathbf{a}_\theta| \leq \delta\|\mathbf{w}\|$, we have

$$|\mathbf{w}^H \bar{\mathbf{a}}_\theta - 1| \leq |\mathbf{w}^H \mathbf{a}_\theta - 1| + \delta\|\mathbf{w}\| \leq c_\theta \quad (9)$$

This completes the proof. \square

Since the DoA θ_0 contains estimation error, we propose to introduce multiple inequality constraints at nearby angles of θ_0 to improve robustness. Let Θ be a pre-specified discrete angle set, which specifies a desired angle aperture around the target to handle the DoA error, i.e., $\Theta = \theta_0 + \{-5^\circ, 0^\circ, 5^\circ\}$. Finally, we propose robust constraints for protecting target signal as follows:

$$|\mathbf{w}^H \mathbf{a}_\theta - 1| + \delta\|\mathbf{w}\| \leq c_\theta, \quad \forall \theta \in \Theta, \quad (10)$$

Inequality constraints (10) try to form a wide aperture beam around θ_0 to robustly protect the target signal, and the true spatial response for each $\theta \in \Theta$ is bounded (Proposition 1).

B. Robustness against Inaccurate Estimation of \mathbf{R}_u

There are two ways to improve the robustness to the inaccurate estimation of \mathbf{R}_u . One is to exploit the inherent structure of \mathbf{R}_u and develop an efficient estimator for \mathbf{R}_u from finite samples, like covariance matrix reconstruction approaches [24]–[26]. The other approach is to exploit the a priori knowledge of the presumed steering vectors for interferences and impose robust constraints to suppress interferences even without \mathbf{R}_u . Following the second way, we propose to impose the following inequality constraints for interference suppression,

$$|\mathbf{w}^H \mathbf{a}_\phi| + \delta\|\mathbf{w}\| \leq c_\phi, \quad \forall \phi \in \Phi_k, \quad \forall k, \quad (11)$$

where Φ_k is a pre-defined discrete angle set for the interference k based on the corresponding DoA estimation θ_k , i.e., $\Phi_k = \theta_k + \{-5^\circ, 0^\circ, 5^\circ\}$, and $c_\phi \geq 0$ specifies an allowable amplification for angle ϕ . Similar to Proposition 1, constraints (11) implies an upper bound for the true spatial response $\mathbf{w}^H \bar{\mathbf{a}}_\phi$ given in Proposition 2.

Proposition 2. Suppose $\mathbf{a}_\phi = \bar{\mathbf{a}}_\phi + \Delta\mathbf{a}_\phi$ ($\|\Delta\mathbf{a}_\phi\| \leq \delta$) and $|\mathbf{w}^H \mathbf{a}_\phi| + \delta\|\mathbf{w}\| \leq c_\phi$, then $|\mathbf{w}^H \bar{\mathbf{a}}_\phi| \leq c_\phi$.

Proof. Similar to the proof for Proposition 1, applying the triangle and Cauchy–Schwarz inequalities can complete this proof. \square

Intuitively, constraints (11) try to form a sufficiently wide and bounded null at nearby angles of ϕ_k , which can suppress interferences with robustly regardless the estimation quality of \mathbf{R}_u . The MVDR formulation (4) can be modified by replacing constraint (4b) with constraints (10) and (11), leading to a robust beamformer design. Such beamformer (with $\delta = 0$) was recently proposed and studied in [2], [34], named as ICMV beamformer in short. However, the ICMV beamformer also suffers from a design feasibility issue, i.e., the ICMV formulation may not be feasible when the number of constraints is larger than the number of array elements. In fact, the design of beamformer under limited DoF condition is not just a challenge for the ICMV, but also for other multiple constraints based beamformer design like the LCMV beamformer or other linear constraints based beamformers [32], [33]. The key question is whether there is a feasible way to impose arbitrary number of robust constraints when the number of array elements is fixed? In what follows, we provide a positive answer affirmatively by proposing a minmax robust beamforming formulation.

C. Limited DoF

In this subsection, we introduce a penalization criterion for constraints (11). The proposed design criterion always enables a feasible beamformer design (under mild conditions, see Proposition 3) while suppressing multiple interferences robustly. From the physical meaning of constraints (11), we know they attempt to bound the spatial responses at several potential angles of interferences. Instead of specifying fixed levels c_ϕ which could cause a design feasibility issue, we introduce an extra optimization variable $\epsilon = [\epsilon_1, \epsilon_2, \dots, \epsilon_K]^T \in \mathbb{R}^K$ on the right hand sides of constraints (11) to control the levels of spatial responses. We propose the following min-max optimization criterion for suppressing multiple interferences in a robust manner:

$$\begin{aligned} \min_{\mathbf{w}, \epsilon} \quad & \max_k \{\gamma_k \epsilon_k\} + \text{Other objectives} \\ \text{s.t.} \quad & |\mathbf{w}^H \mathbf{a}_\phi| + \delta\|\mathbf{w}\| \leq \epsilon_k c_\phi, \quad \forall \phi \in \Phi_k, \quad \forall k, \\ & \text{Other feasible constraints.} \end{aligned} \quad (12)$$

In (12), $\{\gamma_k\}$ are user-specified interference suppression parameters, interference with larger γ_k has higher priority to be suppressed. Suppose $c_\phi > 0, \forall \phi \in \Phi_k, \forall k$, criterion (12) always enables a feasible design for \mathbf{w} by setting the values of $\{\epsilon_k\}$ large enough.

D. Proposed P-ICMV Beamformer

Finally, combine the discussions in Subsections III-A, III-B, and III-C, the proposed P-ICMV formulation is

$$\begin{aligned} \min_{\mathbf{w}, \epsilon} \quad & \mathbf{w}^H \mathbf{R} \mathbf{w} + \mu \max_k \{\gamma_k \epsilon_k\} \\ \text{s.t.} \quad & |\mathbf{w}^H \mathbf{a}_\theta - 1| + \delta \|\mathbf{w}\| \leq c_\theta, \quad \forall \theta \in \Theta, \\ & |\mathbf{w}^H \mathbf{a}_\phi| + \delta \|\mathbf{w}\| \leq \epsilon_k c_\phi, \quad \forall \phi \in \Phi_k, \quad \forall k. \end{aligned} \quad (13)$$

In (13), \mathbf{R} can be the estimated noise-only covariance matrix or the estimated noise-plus-interference correlation matrix, and $\mu \geq 0$ is a trade-off parameter for noise and interference suppression. The P-ICMV formulation (13) has an extra optimization variable ϵ which makes the upper bound on $|\mathbf{w}^H \mathbf{a}_\phi|$ adjustable. The number of constraints for interference suppression is no longer limited by the DoF. The feasibility can be achieved by setting ϵ large enough. Thus if constraints for angle $\theta \in \Theta$ are nonempty, the P-ICMV beamformer is able to generate a feasible design with bounded distortion for arbitrary number of interferences. To strictly ensure P-ICMV formulation (13) being able to handle arbitrary number of interferences with bounded distortion, we provide the following sufficient condition in Proposition 3.

Proposition 3. Let $\mathbf{A} \in \mathbb{C}^{M \times |\Theta|}$ be the matrix stacked by $\mathbf{a}_\theta, \forall \theta \in \Theta$, suppose $\text{rank}(\mathbf{A}) = |\Theta|$ and $\delta \leq \frac{\min_\theta c_\theta}{\sqrt{\mathbf{1}^H (\mathbf{A}^H \mathbf{A})^{-1} \mathbf{1}}}$. Then problem (13) is always feasible.

Proof. Consider the value of $\|\mathbf{w}\|$ subject to $\mathbf{A}^H \mathbf{w} = \mathbf{b}$, where $\mathbf{b} \in \mathbb{C}^{|\Theta|}$ is a complex vector. By the method of Lagrange multipliers, $\mathbf{w}^* = \mathbf{A}(\mathbf{A}^H \mathbf{A})^{-1} \mathbf{b}$ achieves the minimal $\|\mathbf{w}\|$, given as $\|\mathbf{w}^*\| = \sqrt{\mathbf{b}^H (\mathbf{A}^H \mathbf{A})^{-1} \mathbf{b}}$. If exists \mathbf{b} such that $|\mathbf{b}_\theta - 1| + \delta \sqrt{\mathbf{b}^H (\mathbf{A}^H \mathbf{A})^{-1} \mathbf{b}} \leq c_\theta, \quad \forall \theta \in \Theta$, then \mathbf{w}^* is a feasible solution for problem (13). Setting $\mathbf{b} = \mathbf{1}$ completes the proof. \square

In short, we summarize several interesting properties of the P-ICMV formulation (13) in the following Remarks.

Remark 1 (Bounded Spatial Responses). By Propositions 1 and 2, if $\|\Delta \mathbf{a}_\theta\| \leq \delta$, then any feasible solution (\mathbf{w}, ϵ) of problem (13) has a bounded signal distortion, $1 - c_\theta \leq |\mathbf{w}^H \bar{\mathbf{a}}_\theta| \leq 1 + c_\theta, \forall \theta \in \Theta$. Similarly, spatial response for each interference is softly bounded by an adjustable parameter ϵ_k , $|\mathbf{w}^H \bar{\mathbf{a}}_\phi| \leq \epsilon_k c_\phi, \forall \phi \in \Phi_k$.

Remark 2 (DoF Allocation). Penalty function $\mu \max_k \{\gamma_k \epsilon_k\}$ enables P-ICMV beamformer to intelligently allocate DoF to suppress the intended interference with larger weight γ_k . This allows selective interference suppression, i.e., larger weight can be applied on interferences with higher degree of annoyance.

In practice, the level of robustness can differ in situations, e.g., more robustness on DoA errors should be introduced if DoA estimations are bad, more robustness on SD are necessary if preserving target signal is the central task. Hence, an appropriate robust beamformer should enable different robustness preferences in different situations. Recall the P-ICMV formulation (13), it has several model parameters to be specified, i.e., $\Theta, \{\Phi_k\}, \{c_\theta\}, \{c_\phi\}, \{\gamma_k\}, \mu, \delta$, these parameters provide a wide range for users to design a robust

beamformer with different considerations. In addition, several existing beamformers, i.e., MVDR, LCMV and DL beamformers, can be regarded as special cases of the P-ICMV formulation, with proper settings for these model parameters. Furthermore, though the P-ICMV formulation is proposed for adaptive beamforming purpose, it can also be used to design a specified static beam pattern by setting $\mathbf{R} = \mathbf{0}$. We illustrate several static beam pattern designs by the P-ICMV formulation in Subsection V-C.

IV. ADMM ALGORITHM FOR P-ICMV BEAMFORMER

Problem (13) is actually a convex second-order cone program (SOCP), and the well-studied interior point method [27] can be used to solve it. However, the computational efficiency of the interior point method is too high in many adaptive beamforming applications such as in an embedded system with limited processing [4], [34], [35]. Recent theoretical progress on the convergence and convergence analysis [36] for the ADMM algorithm provides an alternative way to solve problem (13) in an efficient manner. In this section, we first reformulate (13) as a convex SOCP with smooth objective function and then develop a low computational complexity algorithm to solve it using the ADMM algorithm.

By introducing extra optimization variables $t \in \mathbb{R}$ and $y \in \mathbb{R}$, problem (13) is equivalently reformulated as

$$\begin{aligned} \min_{\mathbf{w}, t, y} \quad & \mathbf{w}^H \mathbf{R} \mathbf{w} + \mu t \\ \text{s.t.} \quad & |\mathbf{w}^H \mathbf{a}_\theta - 1| + \delta y \leq c_\theta, \quad \forall \theta \in \Theta, \\ & |\mathbf{w}^H \mathbf{a}_\phi| + \delta y \leq t c_\phi / \gamma_k, \quad \forall \phi \in \Phi_k, \quad \forall k, \\ & \|\mathbf{w}\| \leq y. \end{aligned} \quad (14)$$

Notice that problems (13) and (14) have the same optimal \mathbf{w}^* , and the optimal $\epsilon_k^*, \forall k$ for problem (13) can be extracted from the optimal (\mathbf{w}^*, y^*, t^*) for problem (14), given as $\max_{\phi \in \Phi_k} \{(|\mathbf{a}_\phi^H \mathbf{w}^*| + \delta y^*) / c_\phi\} \leq \epsilon_k^* \leq t^* / \gamma_k$. To derive the ADMM algorithm for problem (14), we first introduce auxiliary variables $\{y_\theta, z_\theta\}$ and $\{y_\phi, z_\phi\}$ as

$$y_\theta = y, \quad z_\theta = \mathbf{w}^H \mathbf{a}_\theta, \quad \forall \theta \in \Theta, \quad (15a)$$

$$y_\phi = y, \quad z_\phi = \mathbf{w}^H \mathbf{a}_\phi, \quad \forall \phi \in \Phi_k, \quad \forall k. \quad (15b)$$

Then, problem (14) can be equivalently reformulated as

$$\begin{aligned} \min \quad & \mathbf{w}^H \mathbf{R} \mathbf{w} + \mu t \\ \text{s.t.} \quad & |z_\theta - 1| + \delta y_\theta \leq c_\theta, \quad \forall \theta \in \Theta, \end{aligned} \quad (16a)$$

$$|z_\phi| + \delta y_\phi \leq t c_\phi / \gamma_k, \quad \forall \phi \in \Phi_k, \quad \forall k, \quad (16b)$$

$$\|\mathbf{w}\| \leq y, \quad (16c)$$

$$(15a), (15b).$$

Let $L_\rho(\mathbf{w}, y, \{y_\theta, z_\theta\}, t, \{y_\phi, z_\phi\}, \{\eta_\theta, \lambda_\theta\}, \{\eta_\phi, \lambda_\phi\})$ be the augmented Lagrangian function for problem (16) [37]

$$\begin{aligned} L_\rho(\mathbf{w}, y, \{y_\theta, z_\theta\}, t, \{y_\phi, z_\phi\}, \{\eta_\theta, \lambda_\theta\}, \{\eta_\phi, \lambda_\phi\}) &= \mathbf{w}^H \mathbf{R} \mathbf{w} + \mu t \\ &+ \sum_{\theta \in \Theta} \left[\text{Re}\{\lambda_\theta^H (\mathbf{w}^H \mathbf{a}_\theta - z_\theta)\} + \frac{\rho}{2} |\mathbf{w}^H \mathbf{a}_\theta - z_\theta|^2 \right] \\ &+ \sum_{\theta \in \Theta} \left[\eta_\theta (y - y_\theta) + \frac{\rho}{2} (y - y_\theta)^2 \right] \\ &+ \sum_k \sum_{\phi \in \Phi_k} \left[\text{Re}\{\lambda_\phi^H (\mathbf{w}^H \mathbf{a}_\phi - z_\phi)\} + \frac{\rho}{2} |\mathbf{w}^H \mathbf{a}_\phi - z_\phi|^2 \right] \\ &+ \sum_k \sum_{\phi \in \Phi_k} \left[\eta_\phi (y - y_\phi) + \frac{\rho}{2} (y - y_\phi)^2 \right]. \end{aligned}$$

where $\{\lambda_\theta\}$ and $\{\lambda_\phi\}$ are Lagrangian multipliers associated with equality constraints $z_\theta = \mathbf{w}^H \mathbf{a}_\theta, \forall \theta \in \Theta$ and $z_\phi = \mathbf{w}^H \mathbf{a}_\phi, \forall \phi \in \Phi_k, \forall k$, $\{\eta_\theta\}$ and $\{\eta_\phi\}$ are Lagrangian multipliers associated with equality constraints $y_\theta = y, \forall \theta \in \Theta$ and $y_\phi = y, \forall \phi \in \Phi_k, \forall k$, and $\rho > 0$ is the penalty parameter for the ADMM algorithm. Define $\mathbf{x}_1 \triangleq (\mathbf{w}, y)$, $\mathbf{x}_2 \triangleq (\{y_\theta, z_\theta\})$, $\mathbf{x}_3 \triangleq (t, \{y_\phi, z_\phi\})$, and $\boldsymbol{\lambda} = (\{\eta_\theta, \lambda_\theta\}, \{\eta_\phi, \lambda_\phi\})$, then at iteration $r = 0, 1, 2, \dots$, the ADMM algorithm updates all variables as follows:

$$\mathbf{x}_1^{r+1} = \arg \min_{(16c)} L_\rho(\mathbf{x}_1, \mathbf{x}_2^r, \mathbf{x}_3^r, \boldsymbol{\lambda}^r), \quad (17a)$$

$$\mathbf{x}_2^{r+1} = \arg \min_{(16a)} L_\rho(\mathbf{x}_1^{r+1}, \mathbf{x}_2, \mathbf{x}_3^r, \boldsymbol{\lambda}^r), \quad (17b)$$

$$\mathbf{x}_3^{r+1} = \arg \min_{(16b)} L_\rho(\mathbf{x}_1^{r+1}, \mathbf{x}_2^{r+1}, \mathbf{x}_3, \boldsymbol{\lambda}^r), \quad (17c)$$

$$\lambda_\theta^{r+1} = \lambda_\theta^r + \rho(\mathbf{w}^H \mathbf{a}_\theta - z_\theta^{r+1}), \theta \in \Theta, \quad (17d)$$

$$\eta_\theta^{r+1} = \eta_\theta^r + \rho(y - y_\theta), \theta \in \Theta, \quad (17e)$$

$$\lambda_\phi^{r+1} = \lambda_\phi^r + \rho(\mathbf{w}^H \mathbf{a}_\phi - z_\phi^{r+1}), \phi \in \Phi_k, \forall k, \quad (17f)$$

$$\eta_\phi^{r+1} = \eta_\phi^r + \rho(y - y_\phi), \phi \in \Phi_k, \forall k. \quad (17g)$$

The convergence behavior of the above ADMM iterations is given in the following proposition [36].

Proposition 4. Suppose Proposition 3 holds, then iterates $\{\mathbf{w}^r\}$ generated by (17) converge to the optimal \mathbf{w}^* of problem (13) as $r \rightarrow \infty$.

Next, we derive closed-form solutions for subproblems (17a), (17b) and (17c) at each iteration r . We drop the iteration index r for notation simplicity. For convenience of presenting the solutions for subproblems (17b) and (17c), we first give Lemma 1, which provides a closed-form solution for a special type of complex SOCP problem.

Lemma 1. Consider a complex SOCP given as

$$\min_{x,y} a|x|^2 + \text{Re}\{b^H x\} + \alpha y^2 + \beta y \quad \text{s.t. } |x-d| + \delta y \leq c, \quad (18)$$

where $a, \alpha \in \mathbb{R} > 0$, $c, \delta \in \mathbb{R} \geq 0$, $\beta \in \mathbb{R}$, and $b, d \in \mathbb{C}$. Define $\psi = \angle(2ad + b)$ and $r = |\frac{2ad+b}{2a}|$, then the optimal solution (x^*, y^*) for (18) is

$$\begin{aligned} y^* &= \min\left\{-\frac{\beta}{2\alpha}, \frac{2a\delta(c-r) - \beta}{2a\delta^2 + 2\alpha}, c/\delta\right\}, \\ x^* &= d - ce^{j\psi} + e^{j\psi} \max\{c-r, \delta y^*\}. \end{aligned} \quad (19)$$

Proof. See Appendix A. \square

A. Solution for Subproblem (17a)

Subproblem (17a) with respect to \mathbf{w} and y is a convex SOCP, given as

$$\begin{aligned} \min_{\mathbf{w}} \quad & \mathbf{w}^H \mathbf{A} \mathbf{w} + \text{Re}\{\mathbf{b}^H \mathbf{w}\} + \alpha y^2 + \beta y \\ \text{s.t.} \quad & \|\mathbf{w}\| \leq y, \end{aligned} \quad (20)$$

where $\mathbf{A} \succ 0$, \mathbf{b} , α , and β are

$$\mathbf{A} = \mathbf{R} + \frac{\rho}{2} \left(\sum_{\theta \in \Theta} \mathbf{a}_\theta \mathbf{a}_\theta^H + \sum_k \sum_{\phi \in \Phi_k} \mathbf{a}_\phi \mathbf{a}_\phi^H \right), \quad (21)$$

$$\mathbf{b} = -\frac{1}{2} \left[\sum_{\theta \in \Theta} (\lambda_\theta^H \mathbf{a}_\theta - \rho z_\theta^H \mathbf{a}_\theta) + \sum_k \sum_{\phi \in \Phi_k} (\lambda_\phi^H \mathbf{a}_\phi - \rho z_\phi^H \mathbf{a}_\phi) \right],$$

$$\alpha = (|\Theta| + \sum_k |\Phi_k|) \frac{\rho}{2}, \beta = \sum_{\theta \in \Theta} \eta_\theta - \rho y_\theta + \sum_k \sum_{\phi \in \Phi_k} \eta_\phi - \rho y_\phi.$$

Problem (20) has a specific structure, whose optimal solution can be obtained in a closed-form based on bisection search. Details are provided in Lemma 2.

Lemma 2. Let eigenvalue decomposition of \mathbf{A} as $\mathbf{U} \boldsymbol{\Lambda} \mathbf{U}^H$, then the optimal (\mathbf{w}^*, y^*) for problem (20) is

$$\begin{cases} y^* = 0, \mathbf{w}^* = \mathbf{0}, & \text{if } \beta \geq \|\mathbf{b}\|, \\ y^* = -\frac{\beta}{2\alpha}, \mathbf{w}^* = \mathbf{w}(y^*), & \text{if } \beta < \|\mathbf{b}\|, \|\mathbf{A}^{-1} \mathbf{b}\| \leq -\frac{\beta}{\alpha}, \\ f(y^*) = 1, \mathbf{w}^* = \mathbf{w}(y^*), & \text{otherwise,} \end{cases}$$

where $\mathbf{w}(y) = -\mathbf{U}^H \left[2\boldsymbol{\Lambda} + (2\alpha + \frac{\beta}{y}) \mathbf{I} \right]^{-1} \mathbf{U} \mathbf{b}$, and $f(y)$ is a strictly monotonic decreasing function given in (45). Further, the unique solution for $f(y) = 1$ can be obtained by bisection search for $y \in [\max\{0, -\frac{\beta}{2\alpha}\}, \|\mathbf{A}^{-1} \mathbf{b}\|/2]$.

Proof. See Appendix B. \square

The computational cost for solving problem (20) per iteration includes: computing \mathbf{b} with a complexity $\mathcal{O}(M(|\Theta| + \sum_k |\Phi_k|))$, computing \mathbf{w}^* and y^* with a complexity of $\mathcal{O}(M^2)$, and bisection search for y with a complexity of $\mathcal{O}(\log_2 \frac{1}{\Delta})$, where Δ is the numerical precision. In addition, a one-time computational cost for finding the eigenvalues and eigenvectors of \mathbf{A} with a complexity of $\mathcal{O}(M^{2.376})$ is required, since \mathbf{A} does not change through ADMM iterations. In total, the computation complexity per iteration is $\mathcal{O}(M^2 + M(|\Theta| + \sum_k |\Phi_k|) + \log_2 \frac{1}{\Delta})$.

B. Solution for Subproblem (17b)

Subproblem (17b) is separable over each $(y_\theta, z_\theta), \theta \in \Theta$. Thus each optimal $(y_\theta^*, z_\theta^*), \theta \in \Theta$ can be obtained by individually solving the following problem, given as

$$\begin{aligned} \min_{y_\theta, z_\theta} \quad & a_\theta |z_\theta|^2 + \text{Re}\{b_\theta^H z_\theta\} + \alpha_\theta y_\theta^2 + \beta_\theta y_\theta \\ \text{s.t.} \quad & |z_\theta - 1| + \delta y_\theta \leq c_\theta, \end{aligned} \quad (22)$$

where $a_\theta, b_\theta, \alpha_\theta$, and β_θ are

$$a_\theta = \alpha_\theta = \frac{\rho}{2}, \quad b_\theta = -\lambda_\theta - \rho \mathbf{w}^H \mathbf{a}_\theta, \quad \beta_\theta = -\eta_\theta - \rho y.$$

Problem (22) is a complex SOCP with respect to (y_θ, z_θ) . It has the same mathematical form as the SOCP studied in

Lemma 1. Specify $a = a_\theta$, $b = b_\theta$, $c = c_\theta$, $\alpha = \alpha_\theta$, $\beta = \beta_\theta$, $\psi_\theta = \angle(2a_\theta + b_\theta)$, and $d = 1$, we can obtain the closed-form solution for (y_θ^*, z_θ^*) given as

$$\begin{aligned} y_\theta^* &= \min\left\{-\frac{\beta_\theta}{2\alpha_\theta}, \frac{\delta(2a_\theta c_\theta - |2a_\theta + b_\theta|) - \beta_\theta}{2a_\theta \delta^2 + 2\alpha_\theta}, c_\theta/\delta\right\}, \\ z_\theta^* &= 1 - e^{j\psi_\theta} \min\left\{\frac{|2a_\theta + b_\theta|}{2a_\theta}, c_\theta - \delta y_\theta^*\right\} \end{aligned} \quad (23)$$

The effort to solve for (y_θ, z_θ) involves calculating the inner product $\mathbf{w}^H \mathbf{a}_\theta$ which has a complexity of $\mathcal{O}(M)$ and updating (y_θ, z_θ) which has a complexity of $\mathcal{O}(1)$. The overall complexity, for all $\theta \in \Theta$, is $\mathcal{O}((M+1)|\Theta|)$ per iteration.

C. Solution for Subproblem (17c)

Subproblem (17c) with respect to $\{y_\phi, z_\phi\}$ and t is equivalent to

$$\begin{aligned} \min_{t, \{y_\phi, z_\phi\}} \quad & \mu t + \sum_k \sum_{\phi \in \Phi_k} a_\phi |z_\phi|^2 + \text{Re}\{b_\phi^H z_\phi\} + \alpha_\phi y_\phi^2 + \beta_\phi y_\phi \\ \text{s.t.} \quad & |z_\phi| + \delta y_\phi \leq t c_\phi / \gamma_k, \quad \forall \phi \in \Phi_k, \quad k = 1, \dots, K, \end{aligned} \quad (24)$$

where a_ϕ , b_ϕ , α_ϕ , and β_ϕ are

$$a_\phi = \alpha_\phi = \frac{\rho}{2}, \quad b_\phi = -\lambda_\phi - \rho \mathbf{w}^H \mathbf{a}_\phi, \quad \beta_\phi = -\eta_\phi - \rho y.$$

Problem (24) is a convex SOCP with respect to t and all (y_ϕ, z_ϕ) . By exploiting its special problem structure, we can also solve it in closed-form. In what follows, we will present the way to exploit problem structure to obtain the closed-form solution. For any fixed $\bar{t} \in \mathbb{R}$, problem (24) is separable over each (y_ϕ, z_ϕ) , $\forall \phi \in \Phi_k, \forall k$, given as

$$\begin{aligned} \min_{y_\phi, z_\phi} \quad & a_\phi |z_\phi|^2 + \text{Re}\{b_\phi^H z_\phi\} + \alpha_\phi y_\phi^2 + \beta_\phi y_\phi \\ \text{s.t.} \quad & |z_\phi| + \delta y_\phi \leq \bar{t} c_\phi / \gamma_k. \end{aligned} \quad (25)$$

According Lemma 1, the closed-form for optimal (y_ϕ^*, z_ϕ^*) can be obtained by specifying $b = b_\phi$, $c = \bar{t} c_\phi / \gamma_k$, $\alpha = \alpha_\phi$, $\beta = \beta_\phi$, $\psi_\phi = \angle b_\phi$, and $d = 0$, $\forall \phi \in \Phi_k, \forall k$, given as

$$\begin{aligned} y_\phi^* &= \min\left\{-\frac{\beta_\phi}{2\alpha_\phi}, \frac{\delta(2a_\phi \bar{t} c_\phi / \gamma_k - |b_\phi|) - \beta_\phi}{2a_\phi \delta^2 + 2\alpha_\phi}, \frac{\bar{t} c_\phi}{\gamma_k \delta}\right\}, \\ z_\phi^* &= -e^{j\psi_\phi} \min\left\{\frac{|b_\phi|}{2a_\phi}, \bar{t} c_\phi / \gamma_k - \delta y_\phi^*\right\}. \end{aligned} \quad (26)$$

Notice (y_ϕ^*, z_ϕ^*) is a function of \bar{t} , which implies problem (25) can be reduced to an optimization problem with respect to a single variable t . Hence, the question becomes how to find optimal t^* for the reduced problem. In Lemma 3, we first give the equivalent optimization problem with respect to t , and then in Proposition 5, we show that the optimal t^* can be obtained by sorting a set of real numbers.

Lemma 3. *The optimal t^* for problem (24) can be obtained by solving the following unconstrained convex problem (27)*

$$\min_t \quad \mu t + f(t), \quad (27)$$

where $f(t) \triangleq \sum_k \sum_{\phi \in \Phi_k} f_\phi(t)$ and $f_\phi(t)$ is a convex function defined as

$$f_\phi(t) = \begin{cases} a_{\phi,1} t^2 + b_{\phi,1} t, & t \leq \bar{t}_{\phi,1}, \\ a_{\phi,2} t^2 + b_{\phi,2} t + c_{\phi,2}, & \bar{t}_{\phi,1} < t \leq \bar{t}_{\phi,2}, \\ c_{\phi,3}, & \bar{t}_{\phi,2} < t, \end{cases} \quad (28)$$

and

$$\begin{aligned} a_{\phi,1} &= \frac{\alpha_\phi c_\phi^2}{\gamma_k^2 \delta^2}, \quad b_{\phi,1} = \frac{\beta_\phi c_\phi}{\gamma_k \delta}, \quad c_{\phi,3} = -\frac{b_\phi^2}{4a_\phi} - \frac{\beta_\phi^2}{4\alpha_\phi}, \\ a_{\phi,2} &= \frac{\alpha_\phi a_\phi c_\phi^2}{\gamma_k^2 (\alpha_\phi + a_\phi \delta^2)}, \quad b_{\phi,2} = \frac{\delta a_\phi c_\phi \beta_\phi - \alpha_\phi c_\phi |b_\phi|}{\gamma_k (\alpha_\phi + a_\phi \delta^2)}, \\ c_{\phi,2} &= -\frac{(\delta |b_\phi| + \beta_\phi)^2}{4(\alpha_\phi + a_\phi \delta^2)}, \quad \bar{t}_{\phi,1} = -\frac{\gamma_k (|b_\phi| \delta^2 + \beta_\phi \delta)}{2\alpha_\phi c_\phi}, \\ \bar{t}_{\phi,2} &= -\frac{\gamma_k (\beta_\phi \delta - |b_\phi| \alpha_\phi / a_\phi)}{2\alpha_\phi c_\phi}. \end{aligned} \quad (29)$$

Further, $f(t)$ is a smooth convex function.

Proof. Substituting (26) into (25) can complete the proof. \square

Proposition 5. *Let $\{\tilde{t}_\ell\}$ be an increasing sequence consisted by all $\{\bar{t}_{\phi,1}\}$ and $\{\bar{t}_{\phi,2}\}$, denote $\partial f(t)$ as the derivative of $f(t)$ in Lemma 3. If $\partial f(\tilde{t}_1) > -\mu$, then the optimal t^* for problem (27) is*

$$t^* = -\frac{\sum_k \sum_{\phi \in \Phi_k} b_{\phi,1} + \mu}{2 \sum_k \sum_{\phi \in \Phi_k} a_{\phi,1}}.$$

Otherwise there must exist \tilde{t}_ℓ satisfying $\partial f(\tilde{t}_\ell) \leq -\mu$ and $\partial f(\tilde{t}_{\ell+1}) \geq -\mu$, then the optimal t^* for problem (27) is

$$t^* = -\frac{\sum_{\phi \in \Omega_1} b_{\phi,1} + \sum_{\phi \in \Omega_2} b_{\phi,2} + \mu}{2(\sum_{\phi \in \Omega_1} a_{\phi,1} + \sum_{\phi \in \Omega_2} a_{\phi,2})}, \quad (30)$$

where sets Ω_1 and Ω_2 are defined as

$$\Omega_1 = \{\phi | \bar{t}_{\phi,1} \geq \tilde{t}_{\ell+1}\}, \quad \Omega_2 = \{\phi | \bar{t}_{\phi,1} \leq \tilde{t}_\ell, \bar{t}_{\phi,2} \geq \tilde{t}_{\ell+1}\}.$$

Proof. By Lemma 3, $\partial f(t)$ can be rewritten as

$$\partial f(t) = \sum_k \sum_{\phi \in \Phi_k} \min\{2a_{\phi,1} t + b_{\phi,1}, 2a_{\phi,2} t + b_{\phi,2}, 0\}. \quad (31)$$

By (29) and (31), we know $\partial f(t)$ is a strictly increasing and continuous function for $t \leq \max_\phi \{\bar{t}_{\phi,2}\} \triangleq t_{\max}$ and $\partial f(t) = 0$ for $t \geq t_{\max}$. By the first order optimality condition (the optimal t^* has gradient $-\mu$), problem (27) must have a unique optimal solution $t^* \leq t_{\max}$ such that $\partial f(t^*) = -\mu$. Notice $\partial f(t)$ is a piecewise linear function, the optimal t^* lies on some region with $\partial f(t) = 2at + b$ and $2at^* + b = -\mu$, where $a > 0, b \in \mathbb{R}$ are coefficients to be determined. By (31), if $\partial f(t_{\min}) > -\mu$, $t_{\min} \triangleq \min_\phi \{\bar{t}_{\phi,1}\}$, then the region must be $t \leq t_{\min}$ and hence $a = \sum_k \sum_{\phi \in \Phi_k} a_{\phi,1}$ and $b = \sum_k \sum_{\phi \in \Phi_k} b_{\phi,1}$. Otherwise, there must exist a region within $t_{\min} \leq t \leq t_{\max}$ such that $\partial f(t) = 2at + b$ and $2at^* + b = -\mu$. Sort all $\{\bar{t}_{\phi,1}\}$ and $\{\bar{t}_{\phi,2}\}$ as an increasing sequence $\{\tilde{t}_\ell\}$ and by the strictly increasing property of $\partial f(t)$, the region for $\partial f(t^*) = -\mu$ must be $\tilde{t}_\ell \leq t^* \leq \tilde{t}_{\ell+1}$, where $\partial f(\tilde{t}_\ell) \leq -\mu$ and $\partial f(\tilde{t}_{\ell+1}) \geq -\mu$. In such a case, we have

$$a = \sum_{\phi \in \Omega_1} a_{\phi,1} + \sum_{\phi \in \Omega_2} a_{\phi,2}, \quad b = \sum_{\phi \in \Omega_1} b_{\phi,1} + \sum_{\phi \in \Omega_2} b_{\phi,2},$$

and $\Omega_1 = \{\phi | \bar{t}_{\phi,1} \geq \tilde{t}_{\ell+1}\}$, $\Omega_2 = \{\phi | \bar{t}_{\phi,1} \leq \tilde{t}_\ell, \bar{t}_{\phi,2} \geq \tilde{t}_{\ell+1}\}$. Combining the two cases and setting $t^* = -\frac{b+\mu}{2a}$ can complete the proof. \square

By (26) and Proposition 5, the computational costs for solving problem (24) include the computation of the inner products

$\{\mathbf{w}^H \mathbf{a}_\phi\}$ with a complexity of $\mathcal{O}(M \sum_k |\Phi_k|)$, computing the coefficients in (29) with a complexity of $\mathcal{O}(\sum_k |\Phi_k|)$, sorting $2 \sum_k |\Phi_k|$ points for finding t^* with a complexity of $\mathcal{O}((2 \sum_k |\Phi_k|) \log_2(2 \sum_k |\Phi_k|))$, and extracting $\{y_\phi^*, z_\phi^*\}$ by (26) with a complexity of $\mathcal{O}(\sum_k |\Phi_k|)$. Totally, the complexity is $\mathcal{O}(M \sum_k |\Phi_k| + (2 \sum_k |\Phi_k|) \log_2(2 \sum_k |\Phi_k|) + \sum_k |\Phi_k|)$.

D. Update $\{\lambda_\theta\}$ and $\{\lambda_\phi\}$

See (17d)-(17g). Since the inner products $\mathbf{w}^H \mathbf{a}_\theta$ and $\mathbf{w}^H \mathbf{a}_\phi$ are calculated when solving subproblems (17b) and (17c). The complexity for updating $\{\eta_\phi, \lambda_\theta\}$ and $\{\eta_\phi, \lambda_\phi\}$ is only $\mathcal{O}(|\Theta| + \sum_k |\Phi_k|)$.

E. Proposed ADMM Algorithm

We summarize the proposed ADMM algorithm for the reformulated P-ICMV formulation (16) in Algorithm 1. The total computation complexity of the proposed ADMM algorithm per iteration is $\mathcal{O}(M^2 + (M+1)(|\Theta| + \sum_k |\Phi_k|) + \log_2 \frac{1}{\Delta} + (\sum_k |\Phi_k|) \log_2(\sum_k |\Phi_k|))$. It should be noticed that subproblems (17b) and (17c) (with given t) are separable across $\theta \in \Theta$ and $\phi \in \Phi_k, \forall k$ respectively, parallel implementation for solving these subproblems can further improve the implementation efficiency.

Algorithm 1 An ADMM Algorithm for Problem (16)

Input: $\mathbf{R}, \{\mathbf{a}_\theta\}, \{\mathbf{a}_\phi\}, \{c_\theta\}, \{c_\phi\}, \{\gamma_k\}, \rho, \mu, \delta$

- 1: Compute \mathbf{A} by (21);
- 2: **for** $r = 0, 1, \dots$, until meet some convergence criteria **do**
- 3: Update \mathbf{w}^{r+1} and y^{r+1} by Lemma 2;
- 4: Compute $\{\mathbf{a}_\theta^H \mathbf{w}^{r+1}\}, \{\mathbf{a}_\phi^H \mathbf{w}^{r+1}\}$
- 5: Update $\{z_\theta^{r+1}\}$ and $\{y_\theta^{r+1}\}$ by (23);
- 6: Compute t^{r+1} by Proposition 5;
- 7: Update $\{z_\phi^{r+1}\}$ and $\{y_\phi^{r+1}\}$ by (26);
- 8: Update $\{\eta_\theta^{r+1}, \lambda_\theta^{r+1}\}, \{\eta_\phi^{r+1}, \lambda_\phi^{r+1}\}$ by (17d)-(17g);
- 9: **end for**

Output: The P-ICMV beamformer \mathbf{w}^* .

V. NUMERICAL SIMULATION

In this section, we consider the application of the proposed P-ICMV beamformer in three different scenarios in order to demonstrate its effectiveness. The first is robust adaptive beamforming with antenna array, which is widely used in radar and wireless communication systems. The major challenge for this application is how to robustly handle various errors, including DoA error, SV mismatch error, and covariance estimation error. The robustness of the P-ICMV beamformer against these errors is demonstrated. The second scenario is speech enhancement with microphone array in hearing aids, where the major difficulty is handling multiple interfering speakers with limited number of microphones. The efficiency of suppressing multiple interferences with few number of microphones is verified. The third scenario is beam pattern synthesis for large size array. A specified beam pattern for a 30×30 antenna array is synthesized, where tens of thousands of constraints are needed to achieve the desired beam pattern. The ability of

the P-ICMV formulation to synthesize a desired beam pattern and the efficiency of the proposed ADMM algorithm have been confirmed. For all simulations, the ADMM algorithm stops when both the primal-dual feasibility gap and residual [37] less than 10^{-5} or the number of iterations exceed 10^3 .

A. Robust Adaptive Beamforming with Antenna Array

We consider a uniform linear antenna array of $M = 20$ elements with half wave length spacing. The desired signal is at $\theta_0 = -5^\circ$, and three interfering signals are at $\theta_1 = -60^\circ$, $\theta_2 = -20^\circ$ and $\theta_3 = 45^\circ$ respectively. For each interfering signal, the interference-to-noise ratio (INR) is fixed at 30 dB. The covariance matrix \mathbf{R} is estimated by averaging a finite number of training snapshots, and the desired signal is always present in the snapshots. In all simulations, both the DoA error and the array calibration error are present. Specifically, we assume the estimated DoA $\hat{\theta}_k$ for each source k is uniformly drawn from $\mathcal{U}(\theta_k - 2^\circ, \theta_k + 2^\circ)$. The calibration error is caused by gain and phase perturbation. For each antenna element, the gain and phase perturbation is randomly generated from $\mathcal{N}(1, 0.02^2)$ and $\mathcal{N}(0, (0.01\pi)^2)$ respectively. The beamforming output SINR is used as performance metric and we study the output SINR under different input SNR and number of snapshots conditions. For each simulation condition, the output SINR is averaged by 100 independent Monte Carlo runs.

Four representative robust beamformers in the literature are selected for comparison. One beamformer is the loading sample matrix inversion (LSMI) beamformer [23], with the loading factor set as $10\lambda_{\min}(\mathbf{R})$. The second beamformer is the worst-case beamformer [14] and the robust parameter ϵ in [14] is set to be 3. The third beamformer is the eigenspace beamformer [19] where the number of interferences is assumed to be exactly known. The last beamformer is the SV estimation beamformer [38], whereby parameter of desired signal region is specified as $[\hat{\theta}_0 - 8^\circ, \hat{\theta}_0 + 8^\circ]$. For the P-ICMV beamformer, the discrete angle set Θ is specified as $\Theta = \hat{\theta}_0 + \{-2^\circ, -1^\circ, 0^\circ, 1^\circ, 2^\circ\}$. The corresponding parameter c_Θ is $c_\Theta = \{6, 4, 2, 4, 6\} \times 10^{-1}$. In such a case, the sufficient condition in Proposition 3 for δ is about $\delta \leq 0.24$. Similarly, the angle set Φ_k for each interfering signal k is selected from the region $[-4^\circ, 4^\circ]$, for a total of nine angles centered symmetrically at $\hat{\theta}_k$ with 1° separations. To further capture the environment information for adaptive interference suppression, we use \mathbf{R} and the presumed SVs $\{\mathbf{a}_\phi\}$ to specify parameters $\{c_\phi\}, \{\gamma_k\}$. Precisely, for each Φ_k , c_ϕ is set as $c_\phi = \hat{\sigma}_\phi^{-1} / \max_{\phi \in \Phi_k} \{\hat{\sigma}_\phi^{-1}\}$, where $\hat{\sigma}_\phi^2$ is the estimation of the so-called Capon spectrum [11], defined as $\hat{\sigma}_\phi^2 = 1/\mathbf{a}_\phi^H \mathbf{R}^{-1} \mathbf{a}_\phi$. For $\{\gamma_k\}$, we specify them as $\gamma_k = \beta_k / \max_{k'} \{\beta_{k'}\}$, where $\beta_k = \sum_{\phi \in \Phi_k} \hat{\sigma}_\phi^2$.

In Figs. 1 and 2, the output SINRs of the P-ICMV beamformer are compared with other four beamformers. Parameter μ and δ of the P-ICMV beamformer are set as $\mu = 10\lambda_{\max}(\mathbf{R})$ and $\delta = 10^{-2}$ respectively, while the parameter ρ in the ADMM algorithm is $\rho = 10\mu$. Fig. 1 plots the output SINRs under different SNR condition with 40 snapshots. It can be observed that the P-ICMV beamformer achieves a stable

output SINR and there is about 3dB performance degradation from the optimal SINR among all SNR conditions. However, the other beamformers suffer more performance degradation as SNR increases. Notice the other four beamformers focus on developing robustness against the desired signal's SV mismatch, they perform a little better than the P-ICMV beamformer in low SNR conditions where the estimation error of \mathbf{R} is small. In Fig. 2, the output SINRs under different number of snapshots are compared while the input SNR is fixed at 15dB. The P-ICMV beamformer does not show obvious performance degradation as the number of snapshots decreases while the other beamformers do.

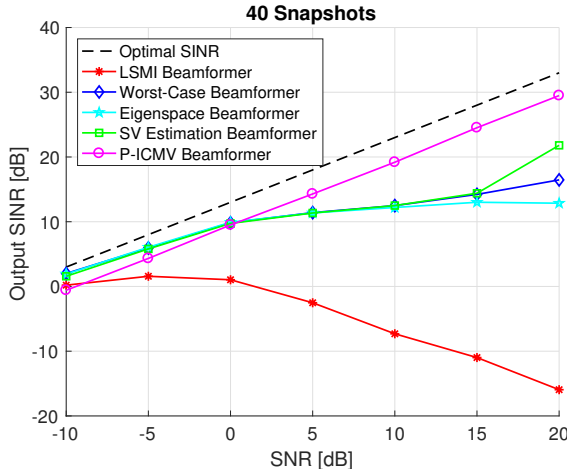


Fig. 1: Output SINRs with different SNRs.

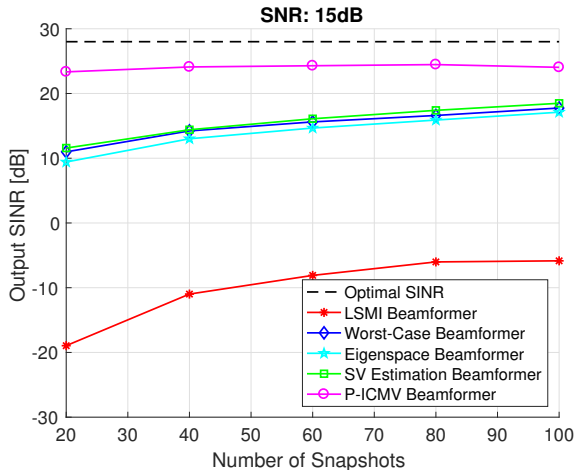


Fig. 2: Output SINRs with different numbers of snapshots.

The impact of the two trade-off parameters μ and δ are studied in Fig. 3. As δ increases, the output SINR slightly increases due to the true spatial response for the target signal direction is bounded with more allowable SV mismatch. However, as δ continues to increase, more DoFs are utilized to guarantee the bounded true spatial responses, and hence the output SINRs deteriorate.

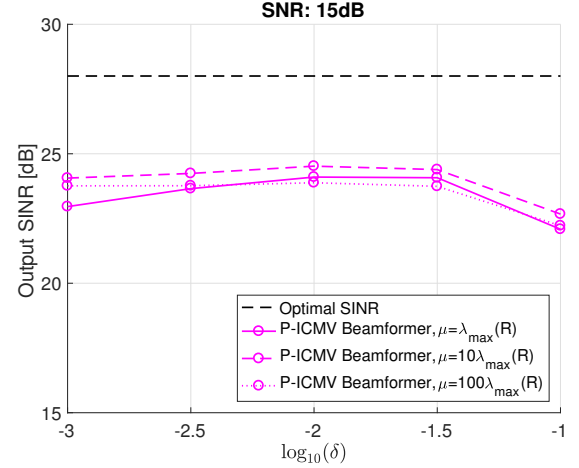


Fig. 3: Output SINRs with different values of μ and δ .

B. Speech Enhancement with Microphone Array

In this subsection, we consider a hearing aids application for speech enhancement with microphone array in a babble noise environment. Similar to the evaluation in [1], [2], two minimum variance-based beamformers: the LCMV and ICMV beamformers are selected for comparison. A rectangular room of size 12.7m \times 10m with height 3.6m is used for simulating the acoustic environment and the reverberation time is set to be 0.6 second. The room impulse responses (RIRs) is generated by the so-called image method [39]. We specify the hearing aids wearer located at the center of the room, each hearing aid has 2 microphones with 7.5mm spacing. The front microphone of the left is set as the reference microphone. The head shadow effect of the listener is also taken into account through using the measurement of the head-related relative transfer functions of the hearings aids on a mannequin. The simulated acoustic environment is illustrated in Fig. 4.

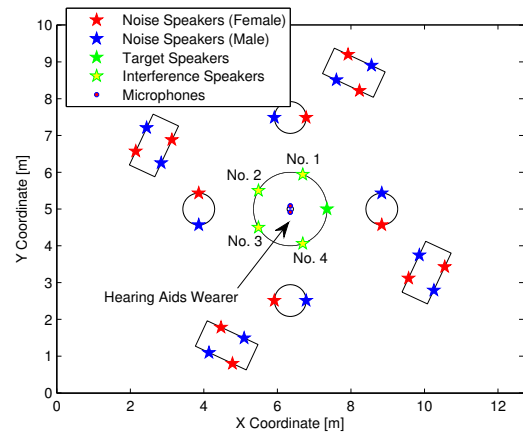


Fig. 4: Simulated acoustic environment.

In the room, there are one target source and four interference sources. The target and interference sources are represented by speakers 1m away from the listener. The target is at 0° and interferences are at $\pm 70^\circ$ and $\pm 150^\circ$ (corresponds to No. 1

to 4 in Fig. 4). The background babble noise is simulated using 24 speakers at different locations. All speakers and hearings aids microphones are in the same horizontal plane at a height of 1.2m. All speakers' speech signals are taken from the TIMIT database [40]. For each speaker, there is 0.5 second silence between each sentence and the speech lasts 25 seconds. In the beginning 3 seconds, only those babble speakers are active and such time segment is utilized for estimating the noise correlation matrix \mathbf{R} by sample averaging. The input signal-to-noise (SNR) at the reference microphone is set at 10dB and signal-to-interference ratio (SIR) for each interference is set at -3dB. The audio signals are sampled at 16kHz and a 1024-point FFT with 50% overlap is used to transform the signals into the time-frequency domain. In the simulation, anechoic ATFs and DoAs of each sources are assumed known.

Since there are in total 5 sources but only 4 microphones, the LCMV and ICMV beamformers can only have constraints on 3 interferences besides the target. We use "Setup i , $i = 1, 2, 3, 4$ " to denote the setting in which interferer i is ignored and other remaining interferences are suppressed with the corresponding constraints. Specifically, define index set $T_i = \{1, 2, 3, 4\}/i$, the LCMV beamformer formulation with setup i is

$$\min_{\mathbf{w}} \mathbf{w}^H \mathbf{R} \mathbf{w} \quad \text{s.t.} \quad \mathbf{w}^H \mathbf{a}_{\theta_0} = 1, \\ \mathbf{w}^H \mathbf{a}_{\theta_k} = 0, \quad \forall k \in T_i,$$

where θ_0 is the DoA of the target source and θ_k is the DoA of interferer k . For the ICMV beamformer with setup i , the corresponding formulation is

$$\min_{\mathbf{w}} \mathbf{w}^H \mathbf{R} \mathbf{w} \quad \text{s.t.} \quad |\mathbf{w}^H \mathbf{a}_{\theta_0} - 1|^2 \leq c_{\theta_0}^2, \\ |\mathbf{w}^H \mathbf{a}_{\theta_k}|^2 \leq c_{\theta_k}^2, \quad \forall k \in T_i,$$

where parameter $\{c_{\theta_k}\}$ are all set to be 0.1. As for the P-ICMV beamformer, the corresponding formulation becomes

$$\min_{\mathbf{w}} \mathbf{w}^H \mathbf{R} \mathbf{w} + \mu \max_k \{\gamma_k \epsilon_k\} \\ \text{s.t.} \quad |\mathbf{w}^H \mathbf{a}_{\theta_0} - 1| + \delta \|\mathbf{w}\| \leq c_{\theta_0}, \\ |\mathbf{w}^H \mathbf{a}_{\theta_k}| + \delta \|\mathbf{w}\| \leq \epsilon_k c_{\theta_k}, \quad \forall k,$$

where parameters $\{c_{\theta_k}\}$ are set the same as the ICMV beamformer, $\gamma_k = 1, \forall k$, and $\mu = \lambda_{\max}(\mathbf{R})$. The sufficient condition for δ by Proposition 3 is $\delta \leq 0.63$ and we choose $\delta = 0.01$. The impact of different μ and δ are studied in Figs. 9 and 10. Penalty parameter ρ for the ADMM algorithm is set to be 10μ for all simulations.

TABLE I: IW-SINRI and IW-SD[dB]

Setup	IW-SINRI				IW-SD			
	1	2	3	4	1	2	3	4
LCMV	7.22	-4.19	-0.11	8.37	0.83	2.11	2.02	0.77
ICMV	8.64	-0.88	2.82	8.86	1.18	1.97	1.92	1.12
P-ICMV	9.35				1.15			

The intelligibility-weighted SINR improvement (IW-SINRI) and intelligibility-weighted spectral distortion (IW-SD) are used as performance metrics [41] and compared in Table

I. In all 4 setups, the P-ICMV beamformer achieves more interference and noise suppression than the LCMV and ICMV beamformers in terms of the IW-SINRI metric. Also all three beamformers have similar speech distortion in terms of IW-SD scores. It can be observed that for the LCMV and ICMV beamformers in setups 1 and 4 when one front interference is ignored, the beamformer achieves reasonable interference suppression. However, in setups 2 and 3 when one interference in the rear one is ignored, the beamformer has a poor IW-SINRI. This can be explained from the individual interference suppression levels (ISL) and the corresponding snapshots of the beam patterns. Fig. 5 plots the ISL for the 4 setups. The ISL is defined as

$$\text{ISL} \triangleq 20 \log_{10} \frac{r_{\text{in}}}{r_{\text{out}}},$$

where r_{in} is the root mean square (RMS) of signal at reference microphone and r_{out} is its RMS at beamformer's output. We can see that the P-ICMV beamformers achieves around 10dB ISL for all interferences, while for the LCMV and ICMV beamformers, only the interferences with constraints are well suppressed. The ignored one is either slightly suppressed or even enhanced depending on the setups.

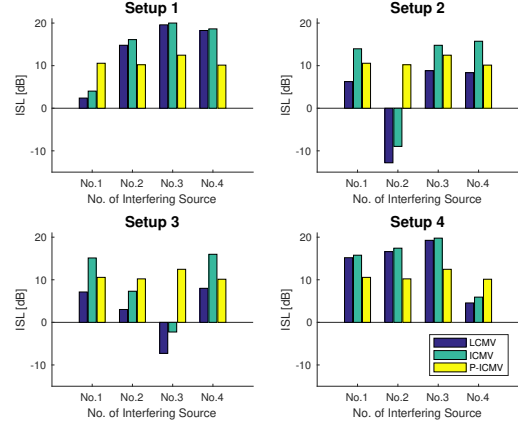


Fig. 5: Individual interference suppression level.

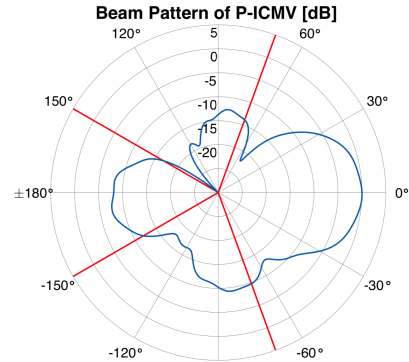


Fig. 6: Beam patterns of P-ICMV at 1000 Hz.

Figs. 6, 7, and 8 plot the beam patterns of the three beamformers at 1000 Hz, where red lines correspond to the 4 interference directions. It can be observed that the P-ICMV

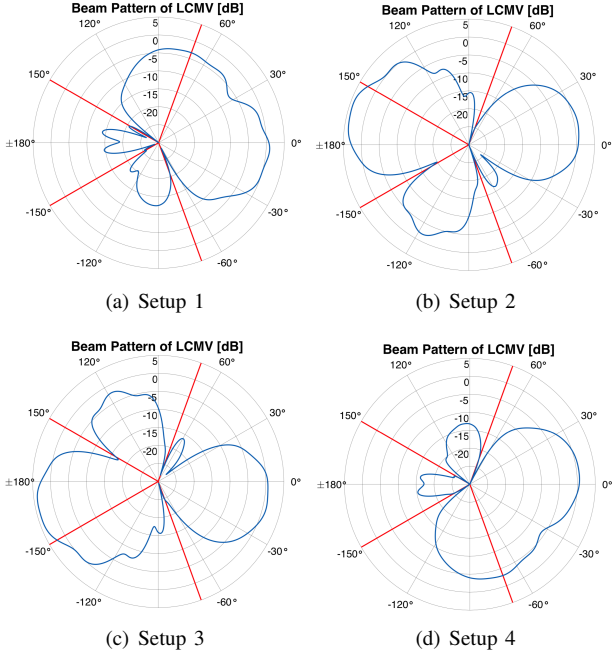


Fig. 7: Beam patterns of LCMV at 1000 Hz.

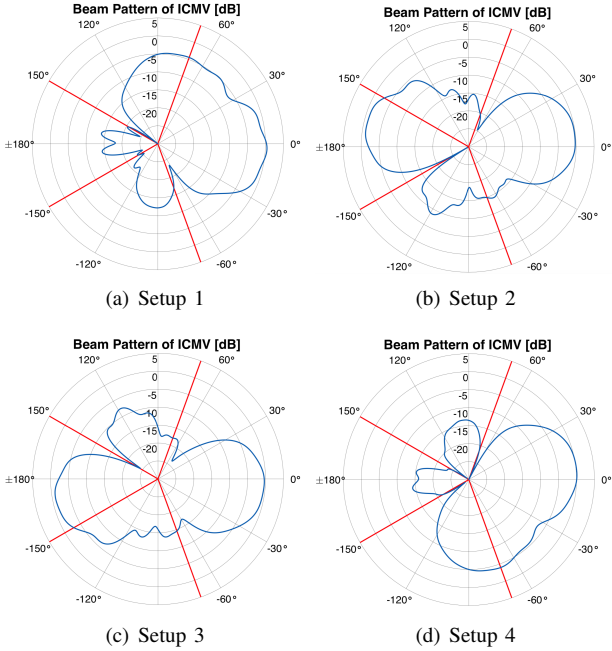
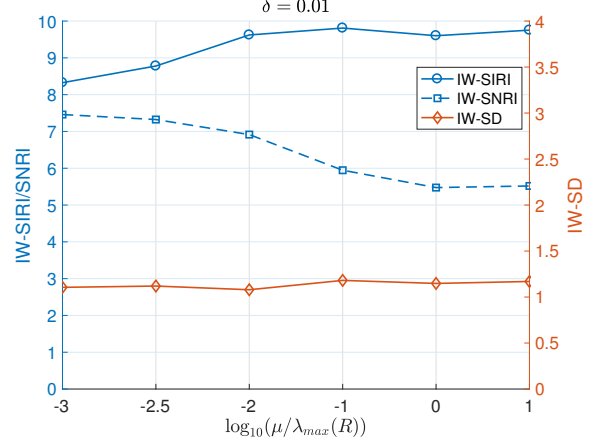
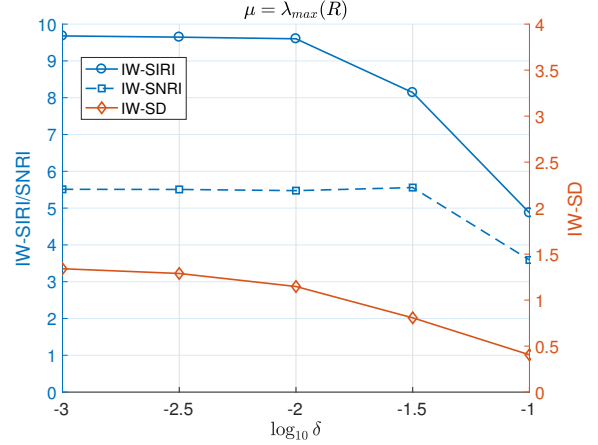


Fig. 8: Beam patterns of ICMV at 1000 Hz.

beamformer has low gain in the spatial responses at all 4 interferences' direction. For LCMV and ICMV beamformers, the ignored interference direction ($\pm 70^\circ$) has reasonable gain control due to the target constraint, but in setups 2 and 3, the ignored interference direction ($\pm 150^\circ$) remains high spatial responses which are even larger than 0dB. In short, when the DoF is limited, the P-ICMV beamformer can automatically handle the target source and all 4 interferences by intelligently allocating the DoF, while the LCMV and ICMV beamformers face a

interference suppression selection problem. Their performance is uncontrollable and is dependent on setups. Furthermore, real listening evaluation on the P-ICMV beamformer is studied in [2], where 12 subjects' listening evaluation demonstrated that the P-ICMV beamformer can significantly improve speech intelligibility in the DoF limited situation.

Fig. 9: IW-SIRIs/SNRIs and IW-SDs with diff. values of μ .Fig. 10: IW-SIRIs/SNRIs and IW-SDs with diff. values of δ .

At last, the performance of the P-ICMV beamformer with different values of μ and δ (with the other one been fixed) are studied in Figs. 9 and 10. To clearly understand the impact of these two parameters, we separately plot IW-SIRI (signal to interference ratio improvement), IW-SNRI (signal to noise ratio improvement), and IW-SD. In Fig. 9 ($\delta = 0.01$), increasing μ gives more priority to interferences suppression. Hence we observe IW-SIRI improves, while IW-SNRI decreases. For a fixed $\mu = \lambda_{\max}(\mathbf{R})$ with different δ (Fig. 10), we can observe that increasing δ can reduce IW-SD, since spatial response for the target signal are always bounded by the level c_θ with more allowable SV mismatch. On the other hand, allocating more DoF to handle SV mismatch would sacrifice the interference and noise suppression performance and hence we observe large IW-SIRI and IW-SNRI decreases as δ increases.

C. Beam Pattern Synthesis

We consider a 30×30 planar antenna array with half wave length spacing. A specified beam pattern with a large region of low side lobes is to be synthesized. Specifically, we use $\vartheta \in [0^\circ, 180^\circ]$ and $\psi \in [-90^\circ, 90^\circ]$ to denote the azimuth and elevation angles. The main lobe of the specified beam pattern is pointed at $\theta_0 = (\vartheta_0, \psi_0) = (90^\circ, 15^\circ)$, and the side lobes (SL) within region $\Phi = \{(\vartheta, \psi) | 0^\circ \leq \vartheta \leq 180^\circ, -90^\circ \leq \psi \leq -10^\circ\}$ are expected to be as low as possible. Such kind of beam pattern is desired in the ground-based radar applications where clutters from low elevation angles are expected to be suppressed as much as possible. To achieve such design requirement, we specify the P-ICMV formulation as follows,

$$\begin{aligned} \min_{\mathbf{w}, \{\epsilon_\phi\}} \quad & \|\mathbf{w}\|^2 + \mu \max_{\phi \in \Phi} \{\epsilon_\phi\} \\ \text{s.t.} \quad & |\mathbf{w}^H \mathbf{a}_\theta - 1| + \delta \|\mathbf{w}\| \leq c_\theta, \quad \forall \theta \in \Theta, \end{aligned} \quad (32a)$$

$$|\mathbf{w}^H \mathbf{a}_\phi| + \delta \|\mathbf{w}\| \leq \epsilon_\phi c_\phi, \quad \forall \phi \in \Phi, \quad (32b)$$

where $\Theta = \{(\vartheta, \psi) | \vartheta_0 - 1^\circ \leq \vartheta \leq \vartheta_0 + 1^\circ, \psi_0 - 1^\circ \leq \psi \leq \psi_0 + 1^\circ\}$ and angle sets Θ and Φ are sampled every 1° for both azimuth and elevation angles.

In the simulation, parameter c_θ is specified as $c_\theta = 0.3 \times (\lceil \vartheta - \vartheta_0 \rceil + \lceil \psi - \psi_0 \rceil + 1)$, $\theta = (\vartheta, \psi) \in \Theta$, where $\lceil \cdot \rceil$ denotes the operation for counting angles difference by unit degree, i.e., $\lceil \pm 1^\circ \rceil = 1$. The sufficient condition in Proposition 3 gives the bound $\delta \leq 1.15$. The value of c_ϕ is fixed the same for all $\phi = (\vartheta, \psi) \in \Phi$ as 0.1. To study the impact of parameters μ and δ , we fix $\mu = 10$ and evaluate the synthesized beam patterns with different choice of δ ($\delta = 10^{-3}, 10^{-2}, 10^{-1}, 10^{-0.5}$). Notice that there are totally 14670 constraints for the specified P-ICMV formulation (32), i.e., $3 \times 3 = 9$ constraints for Θ and $181 \times 81 = 14661$ constraints for Φ . Parameter ρ in ADMM algorithm is set 10^2 , and it only takes few tens of seconds for the ADMM algorithm numerically converge.

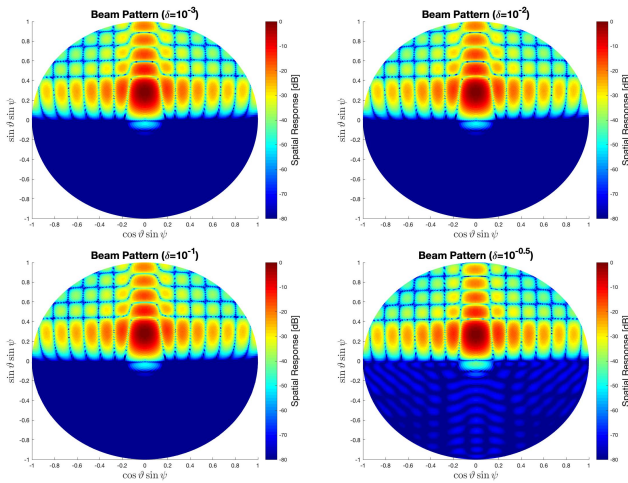


Fig. 11: Synthesized beam patterns with different δ .

The synthesized beam patterns with presumed SVs are plotted in Fig. 11. It can be observed that SL within region Φ have been well suppressed for all choice of δ . However, as compared in Table II, the maximum SL (MSL) and average

SL (ASL) within region Φ with different δ are quite different. Small δ allows more DoF for achieving smaller side lobes but at the cost of increasing $\|\mathbf{w}\|$. For large value of δ , more DoF is allocated to counter the SV mismatch, and hence large MSL and ASL are observed. Furthermore, in the presence of SV mismatch, the levels of true SL are affected by SV mismatch level. To evaluate the impact of δ on the levels of true SL, we assume the SV perturbation consists of gain and phase perturbations, which are randomly generated from $\mathcal{N}(1, \kappa^2)$ and $\mathcal{N}(0, (\kappa\pi/2)^2)$ respectively and $\kappa > 0$ controls the level of SV perturbation. The MSL and ASL with respect to $\delta = 10^{-3}, 10^{-0.5}$ and different κ are compared in Fig. 12, where the MSL and ASL are calculated by averaging 100 independent simulation runs by randomly generating the mismatched SVs. It can be observed that small δ gives lower MSL and ASL when κ is small ($\kappa = 10^{-4}$). As κ increases, large δ achieves lower MSL and ASL since it handles a larger SV mismatch. By Proposition 2, we know constraints (32b) imply that the true spatial response $|\mathbf{w}^H \bar{\mathbf{a}}_\phi| \leq \epsilon_\phi c_\phi, \forall \phi \in \Phi$ for all perturbation satisfy $\|\Delta \mathbf{a}_\phi\| \leq \delta$. In the case of $\|\Delta \mathbf{a}_\phi\| = \delta' > \delta$, the true spatial response is actually bounded by $\epsilon_\phi c_\phi$ and $\|\mathbf{w}\|$,

$$|\mathbf{w}^H \bar{\mathbf{a}}_\phi| \leq |\mathbf{w}^H \mathbf{a}_\phi| + \delta' \|\mathbf{w}\| \leq \epsilon_\phi c_\phi + (\delta' - \delta) \|\mathbf{w}\|.$$

Hence, we observe that a large δ (which has a smaller $\|\mathbf{w}\|$) achieves a smaller MSL/ASL when κ is large (corresponds to large δ').

TABLE II: MSL and ASL [dB]

	$\delta = 10^{-3}$	$\delta = 10^{-2}$	$\delta = 10^{-1}$	$\delta = 10^{-0.5}$
$\ \mathbf{w}\ $	0.0298	0.0297	0.0290	0.0264
MSL	-81.7	-81.6	-80.9	-70.1
ASL	-89.4	-89.4	-88.4	-82.8

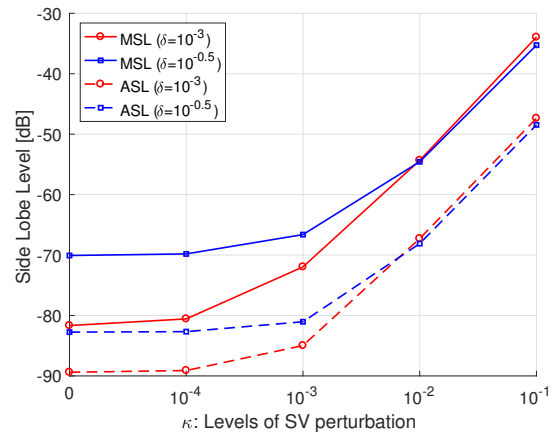


Fig. 12: Side lobe levels with different κ .

VI. CONCLUSION

Robust beamformer design always tries to seek a balance among robustness and beamforming performance, where the central issue lies in how to strike an appropriate balance automatically with limited array DoF. In this paper, we propose a

design of robust beamformer based on convex optimization to address this issue, where a penalization criterion is utilized for intelligently allocate the limited DoF. The proposed P-ICMV formulation makes use of two types of inequality constraints to introduce robustness against various uncertainties and a min-max penalization criterion for handling an arbitrary number of interferences without DoF limitation. Several user-specified parameters are also used in the formulation, which provide a flexible mechanism to achieve different levels of robustness. In addition, a low-complexity iterative algorithm is designed, which can compute the P-ICMV beamformer efficiently even for a large-size array. The P-ICMV beamformer can provide an effective robust solution for challenging applications where DoF is limited and model parameters are inaccurate. The ability to achieve different robustness levels is demonstrated in the simulations.

APPENDIX A PROOF OF LEMMA 1

The proof of Lemma 1 contains two parts. We first prove that, for fixed y with $c - \delta y \geq 0$, problem (18) has closed-form solution given as $x^* = d - ce^{j\psi} + e^{j\psi} \max\{c - r, \delta y\}$, where $\psi = \angle(2ad + b)$ and $r = |\frac{2ad+b}{2a}|$. Then we give the closed-form solution for the optimal y^* .

For any fixed $y \leq c/\delta$, problem (18) becomes

$$\min_{x \in \mathbb{C}} a|x|^2 + \text{Re}\{b^H x\} \quad \text{s.t. } |x - d|^2 \leq \bar{c}^2, \quad (33)$$

where $\bar{c} = c - \delta y \geq 0$. Since problem (33) is a strongly convex problem ($a > 0$), its unique optimal solution is its KKT point. The KKT conditions of problem (33) are

$$2ax + b + 2\lambda(x - d) = 0, \quad (34a)$$

$$\lambda(|x - d|^2 - \bar{c}^2) = 0, \quad (34b)$$

$$|x - d|^2 - \bar{c}^2 \leq 0, \quad (34c)$$

$$\lambda \geq 0, \quad (34d)$$

where λ is the Lagrangian multiplier associating with constraint $|x - d|^2 \leq \bar{c}^2$. If $2ad = -b$, then $x = d$ and $\lambda = 0$ satisfy all conditions in (34) and hence is the optimal solution. Otherwise, condition (34a) (with $x \neq d$) is equivalent to

$$\lambda = -\frac{2ax + b}{2(x - d)} \quad (35)$$

In the next, we replace conditions (34a) by (35) and study conditions (34b) and (34c) with $\lambda > 0$ and $\lambda = 0$ (condition (34d)). If $\lambda > 0$, then conditions (34b) and (34c) hold only when $|x - d|^2 = \bar{c}^2$. This implies $x = d + \bar{c}e^{j\phi}$, where $\phi \in [-\pi, \pi]$ is a rotation angle. Substitute x into (35), we have

$$\lambda = -\frac{2a(d + \bar{c}e^{j\phi}) + b}{2\bar{c}e^{j\phi}} = -\frac{2ade^{-j\phi} + 2a\bar{c} + be^{-j\phi}}{2\bar{c}}.$$

Notice λ is a positive real number, which implies $-(2ad + b)e^{-j\phi}$ is also a positive real number. Based on the fact that rotating any complex number to be a positive real number only holds when the rotation angle takes its negative phase. Hence we have the only choice for $e^{j\phi} = -\frac{2ad+b}{|2ad+b|}$. If $\lambda = 0$, then $x = -\frac{b}{2a}$ and condition (34c) implies $|2ad + b| \leq 2a\bar{c}$ must

hold. Combine the cases for $\lambda > 0$ and $\lambda = 0$, conditions (34a)-(34d) are simplified as

$$x^* = \begin{cases} -\frac{b}{2a}, & \text{if } |2ad + b| \leq 2a\bar{c}, \\ d - \frac{2ad + b}{|2ad + b|}\bar{c}, & \text{otherwise.} \end{cases} \quad (36)$$

Notice the special case that $2ad = -b, x = d$ is also included in (36). Compactly, define $\psi = \angle(2ad + b)$ and $r = |\frac{2ad+b}{2a}|$, we have $-\frac{b}{2a} = d - re^{j\psi}$, and hence (36) can be expressed as

$$\begin{aligned} x^* &= \begin{cases} d - re^{j\psi}, & \text{if } r \leq \bar{c}, \\ d - \bar{c}e^{j\psi}, & \text{otherwise.} \end{cases} \\ &= d + e^{j\psi} \max\{-r, -\bar{c}\} \quad (\bar{c} = c - \delta y) \\ &= d - ce^{j\psi} + e^{j\psi} \max\{c - r, \delta y\}. \end{aligned} \quad (37)$$

This completes the first part of the proof.

Now we prove the optimal y^* for problem (18) also has a closed-form based on (37). Substitute (37) into problem (18) and ignore some constant terms, problem (18) becomes

$$\min_y f(y) \quad \text{s.t. } y \leq c/\delta, \quad (38)$$

where

$$f(y) = a(\max\{c - r, \delta y\})^2 + 2a(r - c)\max\{c - r, \delta y\} + \alpha y^2 + \beta y.$$

Notice $\max\{c - r, \delta y\}$ is a piecewise linear convex function with respect to y and non-decreasing. This implies $f(y)$ is continuous and strongly convex. Then the optimal y^* for (38) must satisfy $\partial f(y^*) = 0$ or $y^* = c/\delta$, where $\partial f(y)$ is the gradient of $f(y)$ given as

$$\partial f(y) = 2a\delta^2 \max\{0, y - \frac{c-r}{\delta}\} + 2\alpha y + \beta. \quad (39)$$

If $\partial f(\frac{c}{\delta}) = \frac{2ar+2\alpha c+\delta\beta}{\delta} \leq 0$, $f(y)$ is strictly decreasing for $y \leq c/\delta$, hence $y^* = c/\delta$ lies on the boundary. Otherwise, we must have $y^* \leq \delta/c$ such that $\partial f(y^*) = 0$. If $2\alpha(c-r) + \beta\delta \geq 0$, we have $\partial f(\frac{c-r}{\delta}) \geq 0$, which implies $f(y^*) = 2\alpha y^* + \beta = 0$ and hence $y^* = -\frac{\beta}{2\alpha}$; otherwise we have $f(y^*) = 2a\delta^2 y^* - 2a\delta(c-r) + 2\alpha y^* + \beta = 0$ and $y^* = \frac{2a\delta(c-r)-\beta}{2a\delta^2+2\alpha}$. In short, define $\lambda_1 = 2\alpha c - 2\alpha r + \delta\beta < \lambda_2 = 2\alpha c + 2ar + \delta\beta$, we have

$$y^* = \begin{cases} y_1 = -\frac{\beta}{2\alpha}, & \text{if } \lambda_1 \geq 0, \\ y_2 = \frac{c}{\delta}, & \text{if } \lambda_2 \leq 0, \\ y_3 = \frac{2a\delta(c-r)-\beta}{2a\delta^2+2\alpha}, & \text{if } \lambda_1 < 0, \lambda_2 > 0. \end{cases} \quad (40)$$

Notice that $\lambda_1 \geq 0$ implies $y_1 = \min_{i=1,2,3}\{y_i\}$, $\lambda_2 \leq 0$ implies $y_2 = \min_{i=1,2,3}\{y_i\}$, and $\lambda_1 < 0, \lambda_2 > 0$ imply $y_3 = \min_{i=1,2,3}\{y_i\}$. Compactly, we have

$$y^* = \min\{-\frac{\beta}{2\alpha}, \frac{2a\delta(c-r)-\beta}{2a\delta^2+2\alpha}, c/\delta\}, \quad (41)$$

This completes the proof.

APPENDIX B
PROOF OF LEMMA 2

We first transform problem (20) into an equivalent form, and then prove Lemma 2 by studying KKT conditions of the transformed problem. Let the eigenvalue decomposition with respect to $\mathbf{A} \succ 0$ as $\mathbf{A} = \mathbf{U}\mathbf{\Lambda}\mathbf{U}^H$, where \mathbf{U} is a unitary matrix stacked by eigenvectors and $\mathbf{\Lambda}$ is a diagonal matrix with diagonal elements corresponding to eigenvalues $\lambda_i > 0, i = 1, 2, \dots, M$. Since for any $\mathbf{w} \in \mathbb{C}^M$, $\|\mathbf{U}^H \mathbf{w}\| = \|\mathbf{w}\|$ always holds, problem (20) can be equivalently transformed as

$$\begin{aligned} \min_{\bar{\mathbf{w}}} \quad & \bar{\mathbf{w}}^H \mathbf{\Lambda} \bar{\mathbf{w}} + \text{Re}\{\bar{\mathbf{b}}^H \bar{\mathbf{w}}\} + \alpha y^2 + \beta y \\ \text{s.t.} \quad & \|\bar{\mathbf{w}}\| \leq y, \end{aligned} \quad (42)$$

where $\bar{\mathbf{b}} = \mathbf{U}\mathbf{b}$. If $(\bar{\mathbf{w}}^*, y^*)$ is optimal for problem (42), then $(\mathbf{U}^H \bar{\mathbf{w}}^*, y^*)$ is optimal for problem (20). The Lagrangian function for problem (42) is

$$L(\bar{\mathbf{w}}, y, \lambda) = \bar{\mathbf{w}}^H \mathbf{\Lambda} \bar{\mathbf{w}} + \text{Re}\{\bar{\mathbf{b}}^H \bar{\mathbf{w}}\} + \alpha y^2 + \beta y + \lambda(\|\bar{\mathbf{w}}\| - y),$$

where $\lambda \geq 0$ is the Lagrangian multiplier associated with the constraint $\|\bar{\mathbf{w}}\| \leq y$. Notice $L(\bar{\mathbf{w}}, y, \lambda)$ is not differentiable at $\bar{\mathbf{w}} = \mathbf{0}$. To study the case for $\bar{\mathbf{w}}^* \neq \mathbf{0}$, we consider $\beta < \|\bar{\mathbf{b}}\|$, which is a sufficient and necessary condition for $\bar{\mathbf{w}}^* \neq \mathbf{0}$ (see Proposition 6). Then, the KKT conditions of problem (42) for $\beta < \|\bar{\mathbf{b}}\|$ are

$$2\mathbf{\Lambda} \bar{\mathbf{w}} + \bar{\mathbf{b}} + \lambda \frac{\bar{\mathbf{w}}}{\|\bar{\mathbf{w}}\|} = \mathbf{0}, \quad (43a)$$

$$2\alpha y + \beta - \lambda = 0, \quad (43b)$$

$$\|\bar{\mathbf{w}}\| \leq y, \quad (43c)$$

$$\lambda \geq 0, \quad (43d)$$

$$\lambda(\|\bar{\mathbf{w}}\| - y) = 0, \quad (43e)$$

If $\lambda = 0$, we have $y = -\frac{\beta}{2\alpha}$ (by (43b)) and $\bar{\mathbf{w}} = -\frac{1}{2}\mathbf{\Lambda}^{-1}\bar{\mathbf{b}}$ (by (43a)). In this case, (43c) holds if $\|\mathbf{\Lambda}^{-1}\bar{\mathbf{b}}\| \leq -\frac{\beta}{\alpha}$, otherwise we must have $\lambda > 0$. For $\lambda > 0$, we have $\|\bar{\mathbf{w}}\| = y$ (by (43e)) and $\lambda = 2\alpha y + \beta$ (by (43b)). Combining these two equalities with (43a), KKT conditions (43a)-(43e) can be reduced as

$$\bar{\mathbf{w}}_i = -\frac{\bar{\mathbf{b}}_i y}{2\lambda_i y + 2\alpha y + \beta}, \forall i, -\frac{\beta}{2\alpha} \leq y = \|\bar{\mathbf{w}}\|. \quad (44)$$

Combining the two equalities in (44), we have

$$\begin{aligned} f(y) &\triangleq \sum_{i=1}^M \frac{|\bar{\mathbf{b}}_i|^2}{(2\lambda_i y + 2\alpha y + \beta)^2} = 1, \\ y &\geq \max\{0, -\frac{\beta}{2\alpha}\} = y_{\min}. \end{aligned} \quad (45)$$

Since $\lambda_i > 0, \forall i$, and $\lambda = 2\alpha y + \beta > 0$, we have $2\lambda_i y + 2\alpha y + \beta > 0$ and hence $f(y)$ is a monotonically decreasing function. Notice $\lambda > 0$ holds only when $\|\mathbf{\Lambda}^{-1}\bar{\mathbf{b}}\| > -\frac{\beta}{\alpha}$ and $\beta < \|\bar{\mathbf{b}}\|$, which implies $f(0) > 1$ if $y_{\min} = 0$ and $f(-\frac{\beta}{2\alpha}) > 1$ if $y_{\min} = -\frac{\beta}{2\alpha}$. Hence we have $f(y_{\min}) > 1$, and there is a

unique root $y^* > y_{\min}$ satisfying $f(y^*) = 1$. On the other hand, consider $f(y^*) = 1$, we have

$$\begin{aligned} y^* &= y^* \sqrt{f(y^*)} = \sqrt{\sum_{i=1}^M \frac{|\bar{\mathbf{b}}_i|^2}{(2\lambda_i + 2\alpha + \beta/y^*)^2}} \\ &\leq \sqrt{\sum_{i=1}^M \frac{|\bar{\mathbf{b}}_i|^2}{(2\lambda_i)^2}} = \|\mathbf{\Lambda}^{-1}\bar{\mathbf{b}}\|/2 \triangleq y_{\max}. \end{aligned} \quad (46)$$

The unique y^* must lie in $[y_{\min}, y_{\max}]$, and can be obtained by bisection search via (45).

Combining the cases for $\beta \geq \|\bar{\mathbf{b}}\|$ and $\beta < \|\bar{\mathbf{b}}\|$, we obtain the solution for problem (20) as follows,

$$\begin{cases} y^* = 0, \mathbf{w}^* = \mathbf{0}, & \text{if } \beta \geq \|\bar{\mathbf{b}}\|, \\ y^* = -\frac{\beta}{2\alpha}, \mathbf{w}^* = \mathbf{w}(y^*), & \text{if } \beta < \|\bar{\mathbf{b}}\|, \|\mathbf{\Lambda}^{-1}\bar{\mathbf{b}}\| \leq -\frac{\beta}{\alpha}, \\ f(y^*) = 1, \mathbf{w}^* = \mathbf{w}(y^*), & \text{otherwise,} \end{cases}$$

where $\mathbf{w}(y) = -\mathbf{U}^H \left[2\mathbf{\Lambda} + (2\alpha + \frac{\beta}{y})\mathbf{I} \right]^{-1} \mathbf{U}\mathbf{b}$ (by (44)). This completes the proof.

Proposition 6. *The optimal $(\bar{\mathbf{w}}^*, y^*)$ for (42) is $(\mathbf{0}, 0)$ if and only if $\beta \geq \|\bar{\mathbf{b}}\|$.*

Proof. Let the objective function of problem (42) be $f(\bar{\mathbf{w}}, y)$. We first prove ‘if’ case by showing $f(\bar{\mathbf{w}}, y) \geq f(\mathbf{0}, 0) = 0$ for any feasible $(\bar{\mathbf{w}}, y)$ if $\beta \geq \|\bar{\mathbf{b}}\|$. Since $\alpha > 0$ and $\beta \geq 0$, we have $y_{\bar{\mathbf{w}}}^* = \arg \min_{\|\bar{\mathbf{w}}\| \leq y} f(\bar{\mathbf{w}}, y) = \|\bar{\mathbf{w}}\|$. Define $\bar{\mathbf{w}}' = \frac{\bar{\mathbf{w}}}{\|\bar{\mathbf{w}}\|}$ and $\epsilon = \|\bar{\mathbf{w}}\| \geq 0$, we have

$$\begin{aligned} f(\bar{\mathbf{w}}, y) &\geq f(\epsilon \bar{\mathbf{w}}', \epsilon) = (\bar{\mathbf{b}}^H \bar{\mathbf{w}}' / \|\bar{\mathbf{b}}\| + \beta)\epsilon + o(\epsilon^2) \\ &\geq (-\|\bar{\mathbf{b}}\| + \beta)\epsilon + o(\epsilon^2) \\ &\geq 0 = f(\mathbf{0}, 0), \end{aligned}$$

where the second inequality is due to Cauchy-Schwartz inequality $\bar{\mathbf{b}}^H \bar{\mathbf{w}}' \geq -\|\bar{\mathbf{b}}\|$, and the third inequality is due to $\beta \geq \|\bar{\mathbf{b}}\|$. Next, we prove ‘only if’ case by contradiction. Suppose $(\bar{\mathbf{w}}^*, y^*) = (\mathbf{0}, 0)$ is optimal for problem (42) and $\beta < \|\bar{\mathbf{b}}\|$. Then, define a feasible solution $(-\epsilon \bar{\mathbf{b}} / \|\bar{\mathbf{b}}\|, \epsilon)$ with $\epsilon > 0$, we have $f(-\epsilon \bar{\mathbf{b}} / \|\bar{\mathbf{b}}\|, \epsilon) = (-\|\bar{\mathbf{b}}\| + \beta)\epsilon + o(\epsilon^2)$. Since $\beta < \|\bar{\mathbf{b}}\|$ implies $(-\|\bar{\mathbf{b}}\| + \beta)\epsilon < 0$. For sufficiently small $\epsilon > 0$, we have $f(-\epsilon \bar{\mathbf{b}} / \|\bar{\mathbf{b}}\|, \epsilon) < 0$ which contradicts the optimality of $\bar{\mathbf{w}}^*$. This completes the proof. \square

REFERENCES

- [1] W. Pu, J. Xiao, T. Zhang, and Z.-Q. Luo, “A penalized inequality-constrained minimum variance beamformer with applications in hearing aids,” in *2017 IEEE Workshop on Applications of Signal Processing to Audio and Acoustics (WASPAA)*, Oct 2017, pp. 175–179.
- [2] J. Xiao, W. Pu, Z.-Q. Luo, and T. Zhang, “Evaluation of the penalized inequality constrained minimum variance beamformer for hearing aids,” in *2018 IEEE International Conference on Acoustics, Speech and Signal Processing (ICASSP)*, April 2018, pp. 3344–3348.
- [3] D. Tse and P. Viswanath, *Fundamentals of wireless communication*. Cambridge university press, 2005.
- [4] S. Doclo, W. Kellermann, S. Makino, and S. E. Nordholm, “Multi-channel signal enhancement algorithms for assisted listening devices: Exploiting spatial diversity using multiple microphones,” *IEEE Signal Processing Magazine*, vol. 32, no. 2, pp. 18–30, March 2015.

- [5] T. Ho, J. McWhirter, A. Nehorai, U. Nickel, B. Ottersten, B. Steinberg, P. Stoica, M. Viberg, and Z. Zhu, *Radar array processing*. Springer Science & Business Media, 2013, vol. 25.
- [6] A. M. Chiang and S. R. Broadstone, "Sonar beamforming system," Jan. 11 2005, uS Patent 6,842,401.
- [7] J. f. Synnevag, A. Austeng, and S. Holm, "Benefits of minimum-variance beamforming in medical ultrasound imaging," *IEEE Transactions on Ultrasonics, Ferroelectrics, and Frequency Control*, vol. 56, no. 9, pp. 1868–1879, September 2009.
- [8] G. Elko, "Microphone array systems for hands-free telecommunication," *Speech communication*, vol. 20, no. 3–4, pp. 229–240, 1996.
- [9] E. Mabande, A. Schad, and W. Kellermann, "Design of robust superdirective beamformers as a convex optimization problem," in *2009 IEEE International Conference on Acoustics, Speech and Signal Processing*, April 2009, pp. 77–80.
- [10] X. Zhang, Z. He, B. Liao, X. Zhang, Z. Cheng, and Y. Lu, "A²RC: An accurate array response control algorithm for pattern synthesis," *IEEE Transactions on Signal Processing*, vol. 65, no. 7, pp. 1810–1824, April 2017.
- [11] J. Capon, "High-resolution frequency-wavenumber spectrum analysis," *Proceedings of the IEEE*, vol. 57, no. 8, pp. 1408–1418, Aug 1969.
- [12] S. A. Vorobyov, "Principles of minimum variance robust adaptive beamforming design," *Signal Processing*, vol. 93, no. 12, pp. 3264 – 3277, 2013, Special Issue on Advances in Sensor Array Processing in Memory of Alex B. Gershman.
- [13] K. Buckley, "Spatial/spectral filtering with linearly constrained minimum variance beamformers," *IEEE Transactions on Acoustics, Speech, and Signal Processing*, vol. 35, no. 3, pp. 249–266, March 1987.
- [14] S. A. Vorobyov, A. B. Gershman, and Z.-Q. Luo, "Robust adaptive beamforming using worst-case performance optimization: a solution to the signal mismatch problem," *IEEE Transactions on Signal Processing*, vol. 51, no. 2, pp. 313–324, Feb. 2003.
- [15] J. Li, P. Stoica, and Z. Wang, "On robust capon beamforming and diagonal loading," *IEEE Transactions on Signal Processing*, vol. 51, no. 7, pp. 1702–1715, July 2003.
- [16] R. G. Lorenz and S. P. Boyd, "Robust minimum variance beamforming," *IEEE Transactions on Signal Processing*, vol. 53, no. 5, pp. 1684–1696, May 2005.
- [17] S. E. Nai, W. Ser, Z. L. Yu, and H. Chen, "Iterative robust minimum variance beamforming," *IEEE Transactions on Signal Processing*, vol. 59, no. 4, pp. 1601–1611, April 2011.
- [18] L. Chang and C. . Yeh, "Performance of dmi and eigenspace-based beamformers," *IEEE Transactions on Antennas and Propagation*, vol. 40, no. 11, pp. 1336–1347, Nov. 1992.
- [19] D. D. Feldman, "An analysis of the projection method for robust adaptive beamforming," *IEEE Transactions on Antennas and Propagation*, vol. 44, no. 7, pp. 1023–1030, July 1996.
- [20] F. Huang, W. Sheng, and X. Ma, "Modified projection approach for robust adaptive array beamforming," *Signal Processing*, vol. 92, no. 7, pp. 1758 – 1763, 2012.
- [21] H. Cox, R. Zeskind, and M. Owen, "Robust adaptive beamforming," *IEEE Transactions on Acoustics, Speech, and Signal Processing*, vol. 35, no. 10, pp. 1365–1376, October 1987.
- [22] B. D. Carlson, "Covariance matrix estimation errors and diagonal loading in adaptive arrays," *IEEE Transactions on Aerospace and Electronic Systems*, vol. 24, no. 4, pp. 397–401, July 1988.
- [23] A. Elnashar, S. M. Elnoubi, and H. A. El-Mikati, "Further study on robust adaptive beamforming with optimum diagonal loading," *IEEE Transactions on Antennas and Propagation*, vol. 54, no. 12, pp. 3647–3658, Dec. 2006.
- [24] Y. Gu and A. Leshem, "Robust adaptive beamforming based on interference covariance matrix reconstruction and steering vector estimation," *IEEE Transactions on Signal Processing*, vol. 60, no. 7, pp. 3881–3885, July 2012.
- [25] H. Ruan and R. C. de Lamare, "Robust adaptive beamforming using a low-complexity shrinkage-based mismatch estimation algorithm," *IEEE Signal Processing Letters*, vol. 21, no. 1, pp. 60–64, Jan 2014.
- [26] L. Huang, J. Zhang, X. Xu, and Z. Ye, "Robust adaptive beamforming with a novel interference-plus-noise covariance matrix reconstruction method," *IEEE Transactions on Signal Processing*, vol. 63, no. 7, pp. 1643–1650, April 2015.
- [27] S. Mehrotra, "On the implementation of a primal-dual interior point method," *SIAM Journal on optimization*, vol. 2, no. 4, pp. 575–601, 1992.
- [28] D. P. Bertsekas, *Nonlinear programming*. Athena scientific Belmont, 1999.
- [29] H. L. Van Trees, *Optimum array processing: Part IV of detection, estimation, and modulation theory*. John Wiley & Sons, 2004.
- [30] B. Widrow, K. Duvall, R. Gooch, and W. Newman, "Signal cancellation phenomena in adaptive antennas: Causes and cures," *IEEE Transactions on Antennas and Propagation*, vol. 30, no. 3, pp. 469–478, May 1982.
- [31] H. Steyskal, "Synthesis of antenna patterns with prescribed nulls," *IEEE Transactions on Antennas and Propagation*, vol. 30, no. 2, pp. 273–279, March 1982.
- [32] D. Marquardt, V. Hohmann, and S. Doclo, "Interaural coherence preservation in multi-channel wiener filtering-based noise reduction for binaural hearing aids," *IEEE/ACM Transactions on Audio, Speech and Language Processing (TASLP)*, vol. 23, no. 12, pp. 2162–2176, 2015.
- [33] E. Hadad, D. Marquardt, S. Doclo, and S. Gannot, "Theoretical analysis of binaural transfer function mvdr beamformers with interference cue preservation constraints," *IEEE/ACM Transactions on Audio, Speech, and Language Processing*, vol. 23, no. 12, pp. 2449–2464, Dec 2015.
- [34] W. C. Liao, M. Hong, I. Merks, T. Zhang, and Z.-Q. Luo, "Incorporating spatial information in binaural beamforming for noise suppression in hearing aids," in *2015 IEEE International Conference on Acoustics, Speech and Signal Processing (ICASSP)*, April 2015, pp. 5733–5737.
- [35] W. C. Liao, Z.-Q. Luo, I. Merks, and T. Zhang, "An effective low complexity binaural beamforming algorithm for hearing aids," in *2015 IEEE Workshop on Applications of Signal Processing to Audio and Acoustics (WASPAA)*, Oct 2015, pp. 1–5.
- [36] M. Hong and Z.-Q. Luo, "On the linear convergence of the alternating direction method of multipliers," *Mathematical Programming*, vol. 162, no. 1, pp. 165–199, 2017.
- [37] S. Boyd, N. Parikh, E. Chu, B. Peleato, and J. Eckstein, "Distributed optimization and statistical learning via the alternating direction method of multipliers," *Foundations and Trends® in Machine Learning*, vol. 3, no. 1, pp. 1–122, 2011.
- [38] A. Khabbazi-basmenj, S. A. Vorobyov, and A. Hassanien, "Robust adaptive beamforming based on steering vector estimation with as little as possible prior information," *IEEE Transactions on Signal Processing*, vol. 60, no. 6, pp. 2974–2987, June 2012.
- [39] J. B. Allen and D. A. Berkley, "Image method for efficiently simulating small-room acoustics," *The Journal of the Acoustical Society of America*, vol. 65, no. 4, pp. 943–950, 1979.
- [40] J. S. Garofolo, L. F. Lamel, W. M. Fisher, J. G. Fiscus, and D. S. Pallett, "DARPA TIMIT acoustic-phonetic continuous speech corpus," 1993.
- [41] A. Spriet, M. Moonen, and J. Wouters, "Robustness analysis of multichannel wiener filtering and generalized sidelobe cancellation for multimicrophone noise reduction in hearing aid applications," *IEEE Transactions on Speech and Audio Processing*, vol. 13, no. 4, pp. 487–503, July 2005.